University of South-Eastern Norway
Faculty of Technology, Natural Sciences and Maritime Sciences

Master's Thesis

Study programme: Master of Science in Micro and Nano Systems Technology

Autumn 2021

Eshita Gurung

Red phosphor in glass

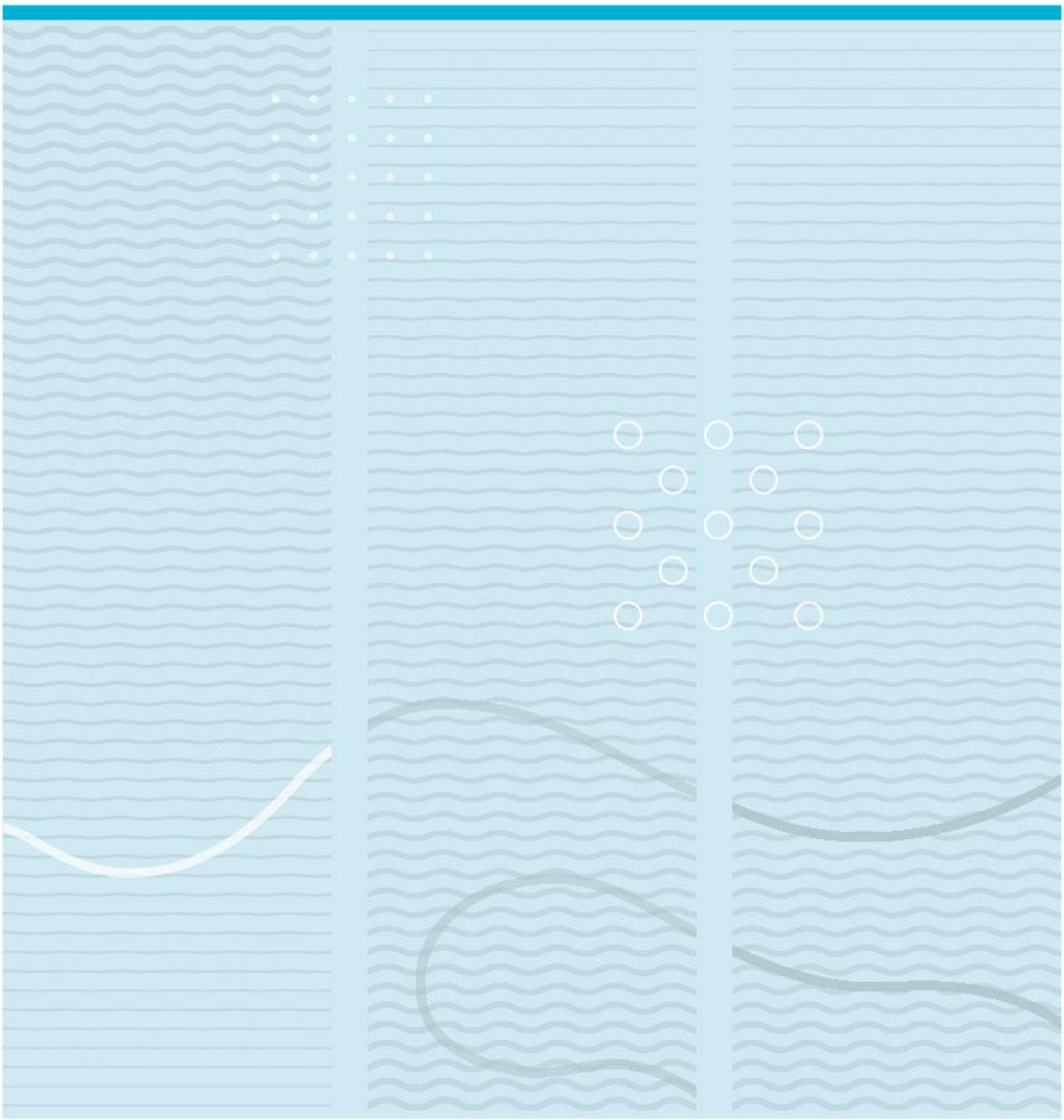

University of South-Eastern Norway
Faculty of Technology, Natural Sciences and Maritime Sciences
Department of Microsystems.
Raveien 215
NO-3184 Borre, Norway

http://www.usn.no

University of South-Eastern Norway

Course: MN-FIN5100 Final Project 2021

Title: Red phosphor in glass

Supervisor: Dr. Xuyuan Chen

Summary

Massive electricity demands every year consume a lot of energy. So, consumption of energy has been a topic that is discussed widely due to alarming environmental threats like global warming. Thus, energy-saving technology is highly demanded.

The lighting consumes a big part of electricity, which motivates the large effort to develop a better efficiency in illumination technology.

Phosphor in glass is a technique that has brought a significant improvement in the solid-state lighting industry in terms of giving the desired color, stability in chemical and thermal properties, is environment-friendly and has a longer lifespan. Thus, it has been commercially accepted in the lighting market and has a start to replace traditional fluorescent lighting.

In this thesis project, phosphor powder was developed in our group, and glass powder was purchased in the market. The host matrix used is yttrium molybdate doped with a red activator, Eu3+: $Y(MoO_4)_3$, and silicate glass powder was used to embed phosphor powder. We aim to optimize the ratio of phosphor over the glass, sintering process for high-performance phosphor glass. The characterization will be followed to guide the analysis and optimization plan.

A scanning Electron microscope (SEM) was used to check the morphological structure of fabricated samples. Excitation and emission spectrum were investigated with Fluorospectrometer. Quantum efficiency was measured using a home-built setup and transmittance was investigated with a UV-VIS spectrophotometer. The excitation

spectrum of phosphor in glass samples had a dominating peak at 395 nm at an emission of 616 nm. The emission peak was dominating at 613 nm when it was excited at a wavelength of 465 nm. The CIE chromaticity coordinates were almost near to the National Television Standard Committee (NTSC) with high color purity. The CIE chromaticity coordinates of NTSC for red phosphor is (x=0.67, y=0.33)[3] and our samples 5% and 10% had (x=0.64,y=0.35) and sample 15% displayed (x=0.65 and y=0.34) respectively. It was noticed that 15% phosphor in glass displayed a brighter violet color when the blue laser is irradiated on the red phosphor sample.

Upon excitation at 465 nm, the quantum efficiency increased with a high phosphor/glass ratio while there was a decrease in transmittance as the phosphor/glass ratio increased.

Acknowledgments

First and foremost I would like to immensely thank my supervisor Dr.Xuyuan Chen and research assistant Fan Chen who has been the guidance, support, and motivation constantly from the very start of my master thesis. I would not have been able to complete my thesis successfully without your patience, valuable suggestions, and feedback, and perseverance regardless of the pandemic situation.

Secondly, I would like to appreciate and express my gratitude to the lab engineer Drs. Birgitte Kasin Hønsval and Ph.D. Chaoqun Cheng helped me with the characterization of my sample during the experiment.

Last but not least I am forever grateful to my family and friends who have been there constantly inspiring and been the pillar of support in bringing the zeal in me to work hard and complete my thesis successfully.

Norway, 13th August 2021

Eshita Gurung

Contents

List of Figures

List of Tables

Chapter 1 Introduction

With the advancement in technology massive amount of energy is consumed and the amount is increasing rapidly every year. According to the statistics, the total electricity demand would be increasing almost double in the upcoming two decades i.e. the net demand for the production of electricity would increase by an average of 2.3% every year, most of which is generated by such as coal, natural gas, oil[4]. Therefore, it leads to serious environmental issues for instance global warming. Global warming which is also termed as the greenhouse effect is the reason behind glacier ice melting, raise in the level of the seawater, occurrence of a hurricane, storms, and flood. Hence, working on an innovative technique for less energy consumption in lighting technology can massively reduce energy usage. This is the major motivation for taking up this project which develops a technology providing an eco-friendly substitute to the former conventional source of lighting.

Timeline of early lighting sources date backs to 70,000 years ago where the prehistoric men used materials like shells, dried grasses, and leaves, and even animal fat for helping in making fire, followed by candles in 200 B.C to gas lamps in the year 1790, the light bulb in 1879, the year 1906 got the light bulb with a tungsten filament, fluorescent tubes were invented during 1938, halogen lamps during 1959 to fluorescent lamps in 1904 to improved lighting system with light-emitting diode(LED) technology were introduced during the year 2008[5].

Conventional sources of light have numerous drawbacks like a shorter life span, more consumption of power, and the addition of pollution to the environment. To prevent these shortcomings, LED technology was introduced which has a lot of advantages/merits over conventional lighting source like it saves 75% less energy than conventional lighting source, are cost-effective, efficient in performance, durable, provide brighter lighting and is eco-friendly [6]. Thus, innovative and improvised technology to the former LED lighting termed as phosphor-converted white light-emitting diode (PC-WLED) or Phosphor in glass came into the picture.

Phosphor is a substance that consists of fluorescent characteristics and emits yellow, green, and red light when they are exposed to some sort of radiation for instance blue

or near UV light[7]. They are divided into two types that are fluorescent and phosphorescent substances where fluorescent substances have the tendency or potentiality of emission of the energy instantly whereas the latter has a delayed emission of energy and stays glowing continuously even when the radiation is off [7].

Phosphor luminescence takes place in 2 different mechanisms and is shown in figure 1-1, i) Luminescence in semiconductors – occurs in donor-acceptor pair[1].

and ii) luminescence in localized centers – occurs between the energy levels where there exists a single number of ions for instance Eu3+ [1].

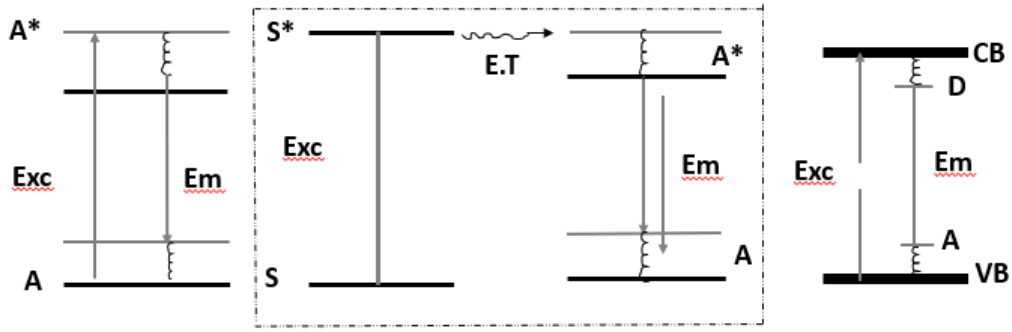

Figure 1-1: Luminescence of phosphor in localized centers (left and middle image) Phosphor luminescence in semiconductors (image at the right).

Where *Exc* – is excitation

Em -is Emission

E. T – is an Energy transfer

CB –is a Conduction band

VB – is the Valence band

1.1 Background literature review on phosphor in glass

With technology development, the traditional organic converter of white-light-emitting diode displayed in figure 1-2 has been replaced by an inorganic color converter displayed in figure 1-3. Inorganic color converters, phosphor was used with silicon, epoxy, and resin. These organic converters when mixed with phosphor lack homogeneity due to their low viscosity had unstable thermal and chemical properties and are extremely sensitive to heat and water[8]. This deteriorated the LED performance like luminescence efficacy and color conversion in the longer run. Thus,

the drawbacks make them not suited for commercial purposes. In contradiction, inorganic converters are with improved performance. There are different inorganic color converters like phosphor ceramics, bulk glass phosphor, glass with quantum dots. Phosphor ceramics requires a large number of phosphor powders making large-scale production extremely expensive[8]. Glass with quantum dot gives less quantum yield and is thermally unstable. Considering all these defects, the phosphor in glass is a considerable substitute and also has been commercially promoted recently[8].

Various phosphors were developed with a glass matrix. Among them, the most popular commercial phosphors are YAG: Ce^{3+} (yellow), LuAG: Ce^{3+}(green), and CASN: Eu^{2+} (red)[8]. Thus, the industry of phosphor-converted white light-emitting diode is advancing and holds the better prospect of replacing the traditional lighting like a fluorescent lamp

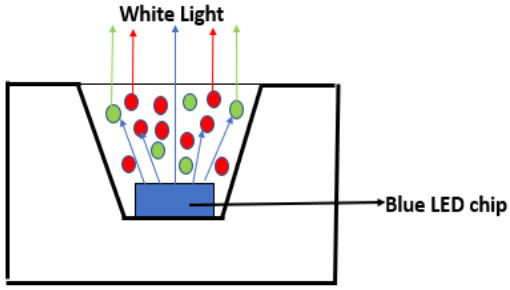

Figure 1-2: Illustration of traditional organic resin phosphor

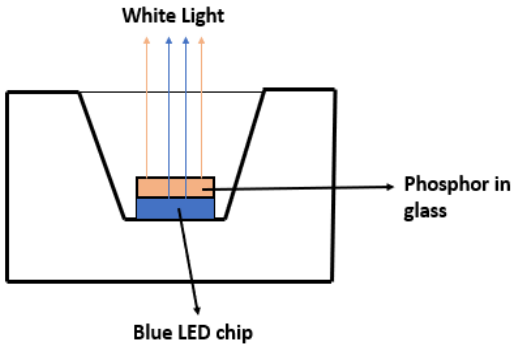

Figure 1-3: Illustration of in-organic color converter phosphor in glass

1.2 Background research on Solid-state lighting

Solid-state lighting technology uses LEDs, OLED (organic light-emitting diode), and light-emitting polymers instead of filaments, plasma, and gas as used in conventional lighting systems[9]. Nowadays, solid-state lights especially LED have been dominating the illumination/lighting market owing to their advantage of a longer lifespan, durable characteristics, and wall-plug efficiency in lighting.

1.3 Working principle/mechanism of LED

The early invention of LED dates back to 1962. Nick Holonyak, Jr. invented the first red LED giving him the title of **"Father of the Light Emitting Diode"** [10]. Soon after that, there was continuous and numerous research for producing better and brighter lighting. There was a huge breakthrough in the year 1993. Nobel prize winner for physics, Shuji Nakamura invented the blue led with extreme brightness capability [11].

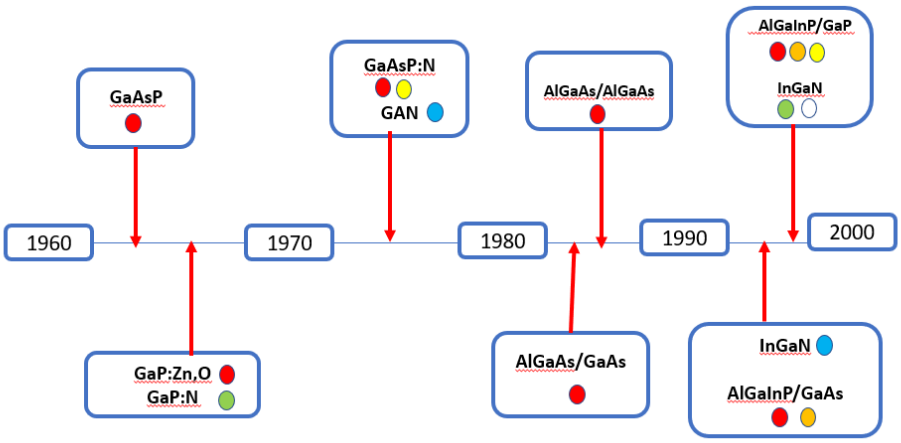

Figure 1-4: Illustration of timeline of semiconductors for LED preparation

Figure 1-4 represents the numerous semiconductors to produce different colors like blue, red, green, yellow LEDs as displayed in the image above.

The working principle of LED can be explained by quantum theory. When the electrons in a LED travel from the higher level of energy states to the ground or lower-level states, energy changes can be realized in the form of photons[12]. When a LED is forward biased, e.g., the positive terminal of the battery is connected to the p-type and the

negative terminal to the n-type. Then both the holes and free electrons will travel towards the junction and recombination of holes and electrons occur as schematically shown in figure 1-5. During this recombination process, the energy is equal to the forbidden energy gap between conduction and valence band.

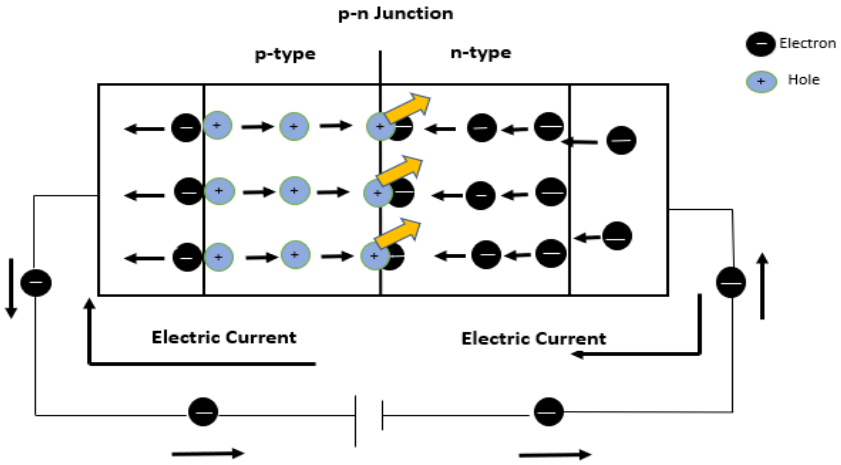

Figure 1-5: Working principle of LED

1.4 White Light Emitting Diode

The white light-emitting diode is considered as the future solid-state light source because of its increasing potential usage in the car's automotive headlight, traffic light, illumination for medical purposes [13]. There are different approaches for the fabrication of white light-emitting diode as mentioned below.

1. Combination of primary colors (Red, Green, and Blue) – in this method blue LED chip made from indium gallium nitride (InGaN) emits blue light which also excites the green and red phosphor and the combination of the blue, red, and green gives the white light [1].
2. Combination of blue LED and yellow phosphor – this has been used in mass production it gives excellent conversion efficiency [1].
3. UV-LED chip and combination of blue, green, and red phosphor [1].

The illustration for the mentioned processes of fabrication of white light-emitting diode is displayed below in figure 1-6.

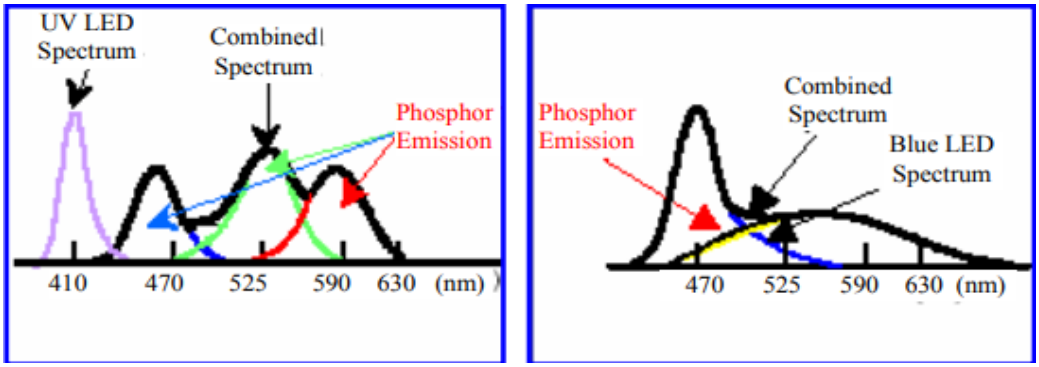

Figure 1-6: a) UV LED chip and blue, red, and green phosphor b) Blue LED chip and yellow phosphor [1]

1.4.1 Optical Characteristics of a white light-emitting diode

There are numbers of parameters to determine the efficiency and quality of light emitted by white light-emitting diode as mentioned below.

1. Internal Quantum Efficiency: it is defined as the ratio of photons emitted to the photons absorbed

$$IQE = \frac{Number\ of\ photons\ emitted}{Number\ of\ photons\ absorbed} \quad [2]$$

2. Absolute Quantum Yield ($PLQY_{abs}$): it is defined as the product of internal quantum efficiency with absorption coefficient [2]

$PLQY_{abs}$ = Internal Quantum Efficiency(Φint) x Absorption Coefficient(ε) [2]

3. Color Rendering Index: defined as the measurement of the capability of the light source to display the original/ true color of a substance/object. The maximum CRI achievable is 100 and for CRI for the indoor lighting should at least achieve equal or more than 80 [2]. Figure 1-7 below illustrates the perfect example of how an object's color can differ according to the varying CRI.

Figure 1-7: Difference in quality of color displayed due to varying (image left) CRI >92, (image right) CRI≈80[2]

4. Correlated color temperature (CCT): As per studies, CCT or correlated color temperature is measured in the unit of Kelvin(K) [2]. It measures whether the emission from the white light is warm light or cool light. In real life, warm white light and cool white light have their field of application as per the customer's needs and requirements [2]. For instance, warm white light is preferred for use in indoor lighting while cool white light is mainly used in outdoor lighting.

   Both warm and cold white light operates and emits at a certain range of temperature as given below.

   1. Warm white light – 3500 K – 4100 K [2]

   2. Cold white light – above 4100 K [2]

5. Luminous Efficacy: It evaluates how efficiently the light produces visible light [2]. It has a unit in lumen/Watt(lm/W).

$$Luminous\ Efficacy = \frac{Total\ luminous\ flux}{Number\ of\ photons Power\ absorbed} \quad [2]$$

1.5 Overview on Luminescence phenomena

The word luminescence was first introduced by a German physicist“Eilhardt Wiedemann” in the year 1988[14]. The material which produces or initiates luminescence is known as luminescent materials or “Phosphors”[15]. The word “Lumen” was derived from Latin which means light and similarly “Phosphor” was derived from a Greek word that means “Light-bearer” [14]. Luminescence occurs when an electron is hit by an external source, it absorbs the energy and gets excited due to which it moves to a higher state from its initial state i.e., ground state. Then, it comes back to the ground state again after releasing energy in the form of radiation or visible light. This is how the process of luminescence occurs.

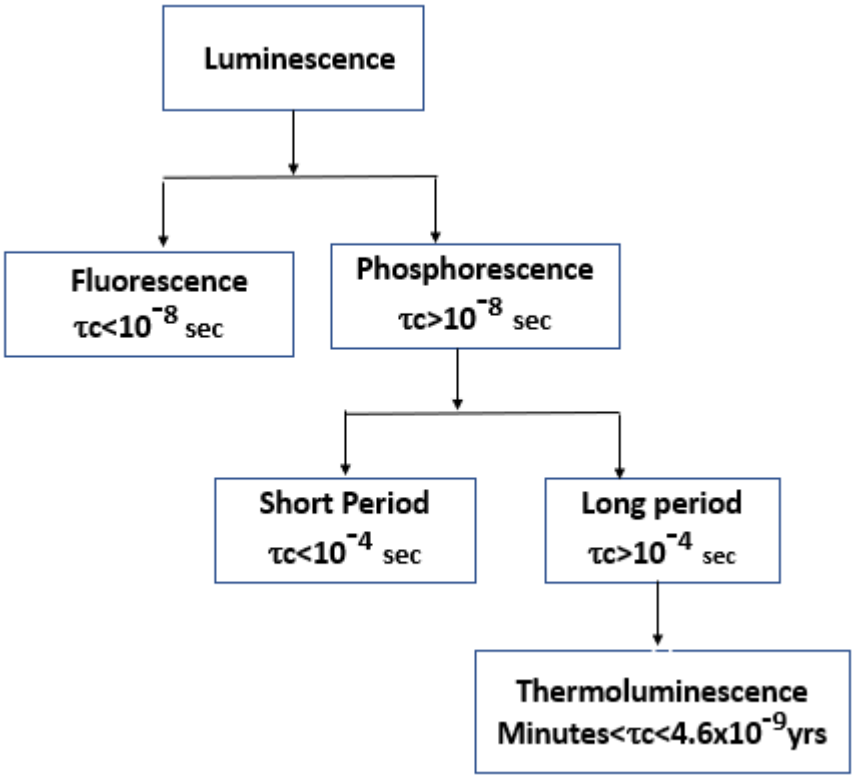

Figure 1-8: Luminescence types based upon timing of emission

Figure 1-8 above represents the different types of luminescence due to different emission timing. Luminescence is sub-divided into two types i.e. Fluorescence and Phosphorescence. Fluorescence is not dependent on temperature while phosphorescence is affected due to temperature and is dependent on it [14]. Phosphorescence is further divided into two, short period and long period. Thermoluminescence has a long time of decay in comparison to other luminescence and ceases to glow even after the excitation has been put off.

There are many types of luminescence as explained below: [14]

1. Chemiluminescence: the process of eruption of light due to chemical reaction.
2. Fluorescence: fluorescent materials absorb light and glow for a certain period.
3. Phosphorescence: Phosphorescent materials glow in the dark and have a longer glowing capacity than fluorescent materials. E.g.: watches and clocks have phosphorescent materials.

4. Photoluminescence: makes use of photons or electromagnetic radiations as excitation sources.
5. Electroluminescence: occurs due to electromagnetic fields applied to the solid or gaseous materials.
6. Radioluminescence: a phenomenon in which the light is made when ground state molecules get excited to the higher state due to collision with high energy particles and also uses radiation.
7. Bioluminescence: is a biochemical type of reaction that can be utilized by living organisms.

As per the study, there are materials whose bandgap is extremely wide. Thus, an external effort is required to initiate the luminescence in them. This is possible via doping such materials where imperfection is introduced into the normal crystal lattice. Hence, it is an important requirement to understand the types of dopants because the dopant added into the host matrix has a huge role in creating a luminescence in the material. There are different types of dopants, and each has its distinct functions.

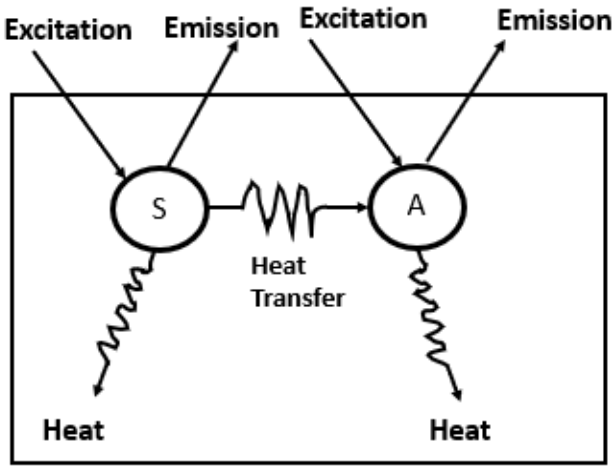

Figure 1-9: Illustration of Luminescence Process

The figure 1-9 represents the process of luminescence that takes place with the help of dopants in the host matrix. There are different types of doping materials used in the practical approach, for instance, Eu^{3+}, Eu^{2+}.

The "A" in the figure is an activator and "S" is known as the sensitizer. Each of these dopants has its function in the luminescence process as described below.

1. Activator: Here, only one dopant ion is doped in the host matrix. The electron from the dopant ion absorbs energy from an external source and travels to a higher state. Then, the same electron returns to its original initial state i.e. ground state by releasing energy in the form of radiation. This type of dopant is also known as the luminescent center[14].
2. Sensitizer: In this type, two dopants are used in a host matrix where one is known as the sensitizer and the other is the activator as displayed in Figure 1-7. The sensitizer's function is to absorb the energy and pass it to the activator dopant which will participate in the process of luminescence and emits light[14].
3. Quenchers: This type of dopant leads to a decrease in the luminescence with the production of heat. Examples of quencher dopants are Fe, Co, etc.
4. **Co-activator**: In this type, the dopant directly doesn't create luminescence but in-directly participates to help the process to occur[14].

1.6 Scope of Thesis research

As mentioned in the introduction section, this project is to develop a technique that can make help in the process of fabrication of a phosphor-converted white light-emitting diode which has tremendous demand in the market due to its various advantages over the traditional lighting system. As per research, the current red phosphor has poor luminescent properties which affect the intensity of luminescence and the lighting market too. Therefore, there is an intensive requirement to develop a red phosphor which is cost-effective and high energy-efficient, (high quantum efficiency), can be manufactured with a simple process, and can be excited with blue or near UV rays. Thus, achieving these requirements is the main aim of the whole project.

1.7 Organization of thesis structure

This section consists of an overview of the structure of thesis content which would help the reader to navigate through the project.

Chapter 1 introduces the reason why this research came into the picture and what is the main motivation and goal of this project. It contains a review of previous research in phosphor-converted white LED, solid-state lighting, and the future of solid-state lighting, Also, the phenomena of luminescence and its classifications are explained.

Chapter 2 presents the materials used in the experiments, explains the fabrication process of phosphor powder and phosphor in glass.

Chapter 3 it consists of the introduction and description of the lab facility used in the project.

Chapter 4 reports the results obtained from the fabrication and characterization and discusses and analyses the results obtained and also reports on the challenges faced.

Chapter 5 consists of the conclusion of this project. In addition, we also describe what could be improved and what is the future scope of this project.

Chapter 2 Fabrication process of phosphor powder, the phosphor in glass

There are various methods for the synthesis of phosphor powder, but it is important to note the fabrication process is not straightforward as there are ample constraints. The constraints mentioned above are mainly due to the physical and chemical properties of the initial raw materials used, limitations involved in the process of synthesis, getting the activator at the required site, cost of production, homogeneity, and reproducibility[16].

The different types of phosphor synthesis are mentioned as follows:

1. Solid-State Reaction: It is a conventional method for the synthesis of luminescent materials. It is a process to obtain polycrystalline material from solid reagents [17]. A very high temperature of 1000° -1500° Celsius is required for the reaction to occur.

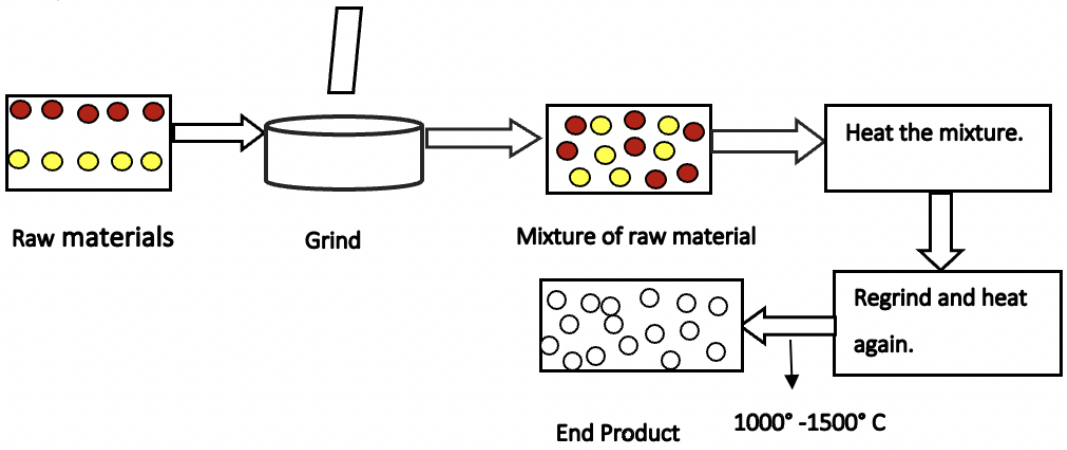

Figure 2-1: Solid state Reaction

Figure 2-1 illustrates the solid-state reaction process to produce luminescent materials where the raw materials and the reagents are grounded together in an agate mortar to get an even mixture and then they are heated/calcined at a temperature of about 1000°Celsius for 5 hours in a ceramic crucible. Subsequently, the mixture is grounded again and re-fired at 1000° Celsius for another 5 hours to get the final product of the luminescent materials [16]. This process was substituted by another process known as the "Sol-Gel Method" because it employs extremely high temperatures, diffusion

between molecules is slow and delayed reaction time. Thus, for this thesis, we have used the Sol-gel method to synthesis the red phosphor powder i.e., Yttrium molybdate which is used as the host matrix and doped with rare-earth ions Eu^{3+} (trivalent europium). Sol-gel technology is comparatively an advanced process and has been successful in the synthesis of oxide coatings, glass, and high critical temperature oxide superconducting materials which is difficult to prepare by the traditional process.

Sol-gel is a wet-chemical technique that employs a high chemically active component termed as the precursor. The initial raw materials are dispersed in the solvent in an aqueous solution, and they undergo a phenomenon known as “Hydrolysis” to form an active monomer [17]. The active monomer is then polymerized, and the formation of sol slowly starts. Post that the solvent is heated and after evaporation of the solvent, a gel-like structure remains back. Finally, after drying and heating treatment, the sample is calcinated under a certain temperature to fabricate the luminescent phosphor powder.

2.1 Equipment and Chemicals Utilised

For the experimental process, the instruments or the equipment and chemicals utilized for the sol-gel technology are described in detail in this following section. The equipment required for the synthesis consists of a hot plate oven with a capacity of heat to approximately 300° Celsius, a beaker for holding the solutions, a magnetic stirrer with a stirring capacity of around 1400 rpm, a high-temperature furnace from Nabertherm company which can heat up to 1750° Celsius with N_2 gas supply pipelines and a ceramic crucible for calcination of phosphor powder. The equipment mentioned is displayed in the figure below.

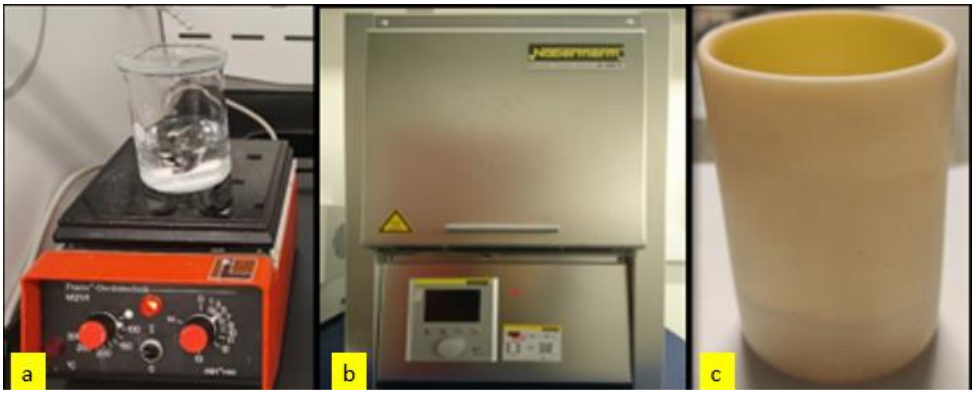

Figure 2-2: (a) Hot plate oven with magnetic stirrer (b) High Temperature furnace (c) Crucible for calcination purpose

Four chemicals were used for the preparation of .002g/mol of phosphor powder and they are mentioned below in the table with their respective molecular weight.

Sl.No	Chemical Name	Molecular Formula	Molecular Weight
1	Citric acid	$C_6H_8O_7$	192.12 g/mol
2	Ammonium molybdate tetrahydrate	$(NH_4)_6Mo_7O_{24}{\cdot}4H2O$	1235.86 g/mol
3	Yttrium (III) nitrate hexahydrate	$Y(NO_3)_3.6H_2O$	383.01 g/mol
4	Europium (III)nitrate pentahydrate	$Eu\ (NO_3)_3{\cdot}5H2O$	428.06 g/mol

Table 2-1: Chemicals used for synthesis of phosphor

2.2 Sol-gel Experiment Details

For the experiment, the first step is the stoichiometric calculation of each chemical according to the target amount of phosphor required. According to the target amount of phosphor required the chemicals were measured respectively in a balance for high accuracy. The target phosphor required for my project was 0.002g/mol hence 1.92 g of citric acid was added to the beaker with a magnetic stirrer and diluted with 80 ml of DI water and heated at a temperature of about 60° C until the acid dissolution. Next,1.06g of ammonium molybdate tetrahydrate solution was added followed by 0.766 g of Yttrium nitrate hexahydrate, and finally, 0.856 gm of Europium nitrate pentahydrate was added. The whole mixture of the solution was covered with a lid and left for heating at 120° C with the magnetic stirrer with approx. speed of 600 rpm for 12 hours for homogenous mixing of the solution.

2.3 Preparation of Gel

After 12 hours of heating the solution with a magnetic stirrer rotating at the speed of 600 rpm, the lid was removed from the beaker and the rotation speed was reduced from 600 rpm to 500 rpm and left at the same temperature i.e 120° C for the evaporation process to occur. After a few durations, a yellow gel formation was noticed as the solution started evaporating. The yellow gel was then pre-calcinated inside the high-temperature furnace.

The figure below illustrates the experimental process for the preparation of phosphor using the Sol-gel Method.

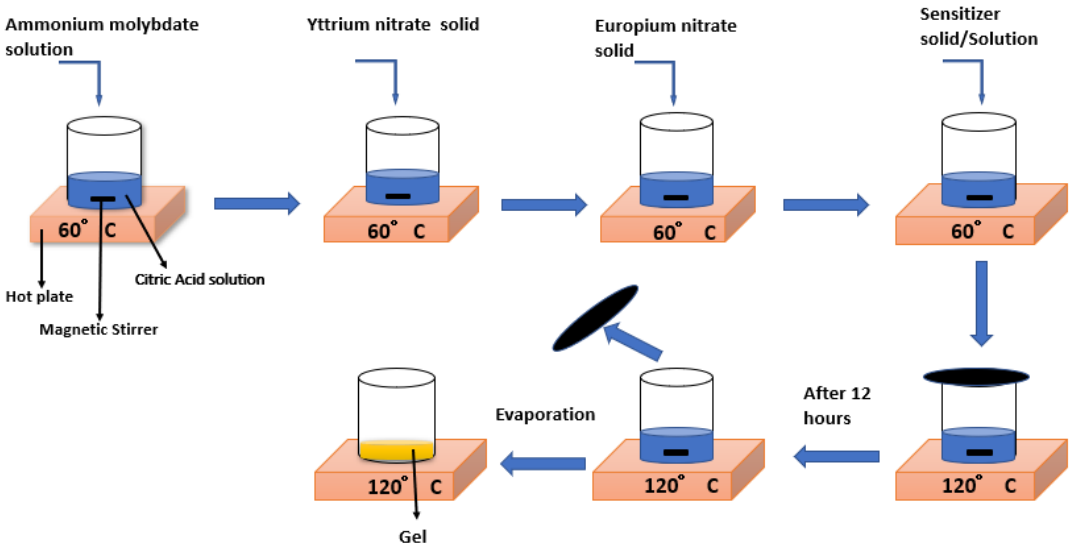

Figure 2-3: Experimental illustration of Sol Gel method

2.4 Final process for fabrication of Phosphor powder

This section consists of the final process employed in the fabrication to obtain phosphor powder. The yellow gel which was left in the beaker post evaporation of the solution was covered again and then pre-calcinated in the high-temperature furnace at 300°C for an hour. After an hour, the formation of a black substance as displayed in the figure was noticed. The black substance was ground for obtaining a homogeneous powder and put inside the temperature furnace for final high-temperature calcination.

Figure 2-4: Black substance formed after pre-calcination of yellow gel

Before, final calcination processes the black powder was put inside the crucible which was pre-heated for dehydration for more than 100° C so that no water residues and impurities are left inside the crucible. The calcination temperature, rate of heating speed, time and atmospheric conditions at which the black powder is calcined is an important factor that would determine the final optical and luminescent properties. Thus, it needs to be studied properly so that the calcination process is done correctly for getting the desired properties from the final product.

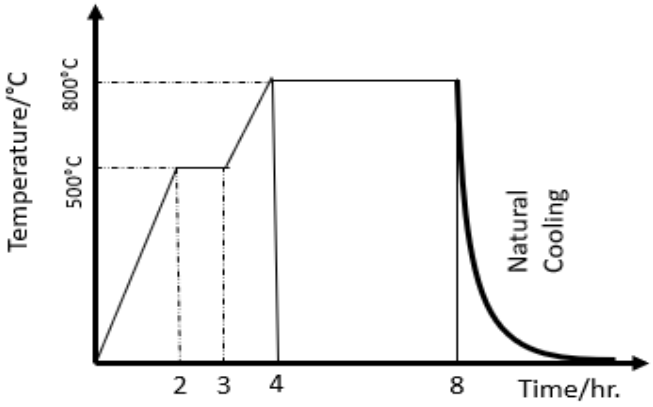

Figure 2-5: Heat curve for calcination process

Figure 2-5 illustrates the heat curve calcination process of phosphor powder where initially the temperature was increased from room temperature to 500° C for 2 hours and then it was kept at 500° C for another 1 hour. After that, the temperature was increased from 500° C to 800° and kept constant for 4 hours. Finally, it was left for natural cooling to room temperature and white fine powders post calcination were observed.

The flow chart of the complete fabrication process with the sol-gel process is displayed below.

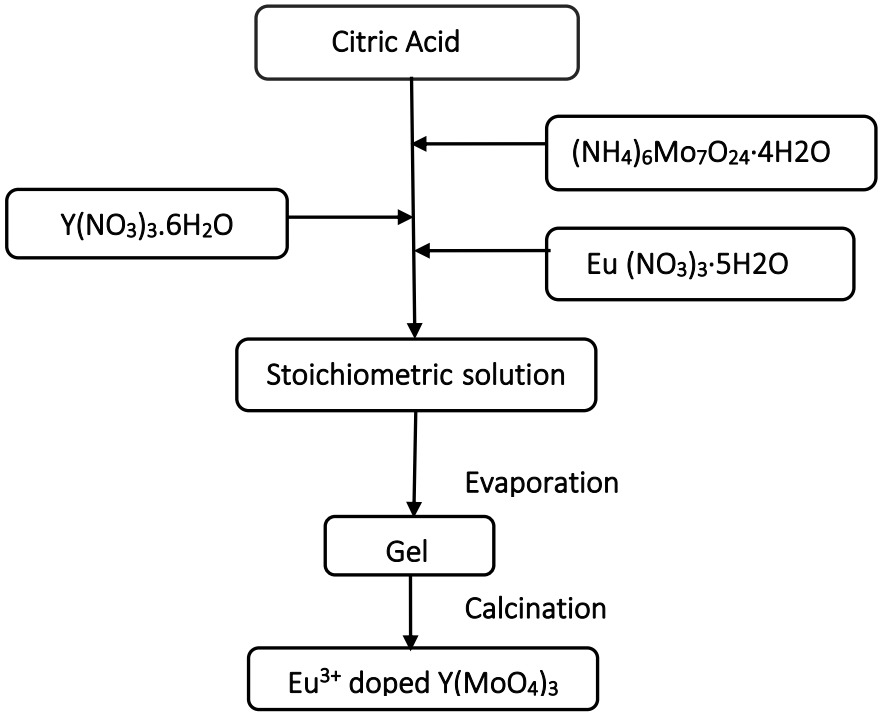

Figure 2-6: Flow chart of Sol Gel process

2.5 Fabrication of Phosphor in Glass

After obtaining the phosphor powder i.e yttrium molybdate doped with Eu^{3+}, the next process was to fabricate the phosphor in Glass. Glass powder was ordered from the Glass forum and the glass powder used is silicate glass powder with 500° C sintering temperature[8] because it has high transparency in the visible range, both chemically and thermally stable and also doesn't consists of ROHS i.e restrictions of hazardous substances [8].

2.5.1 Optimization of phosphor to glass ratio and the sintering time.

We started the fabrication of phosphor in glass by using 50-50 % of phosphor and glass powder and the sintering temperature as tabulated below.

Sl.No	Sintering Temperature	Sintering time
1	25° C – 500 ° C	2 hours
2	500 ° C - 500 ° C	1 hours
3	500° C – 800 ° C	3 hours
4	800° C- 800 ° C	1 hour
5	800° C- 25° C	1 hour
6	Natural cooling	

Table 2.2: Sintering of 50-50% phosphor and glass ratio

This parameter of phosphor ratio and sintering temperature did not give the required results. Figure 2.7 represents the non-homogenous mixture of phosphor and glass where the white material is phosphor, and the darker surface is glass powder. Figure 2.8 represents the sample after the sintering process. The sample was not transparent. Thus, an optimization of the phosphor and glass ratio was done to get better results.

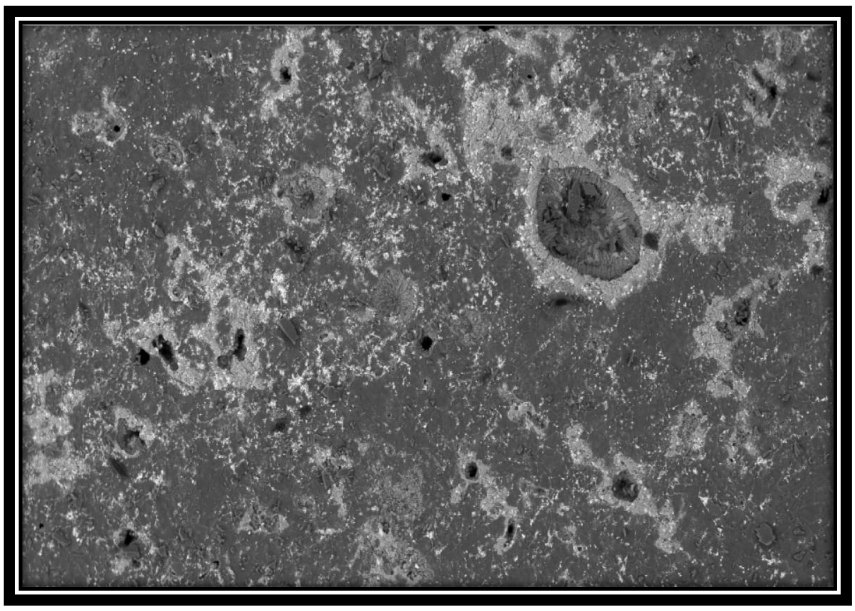

Figure 2.7: SEM morphology of 50-50% of phosphor and glass ratio

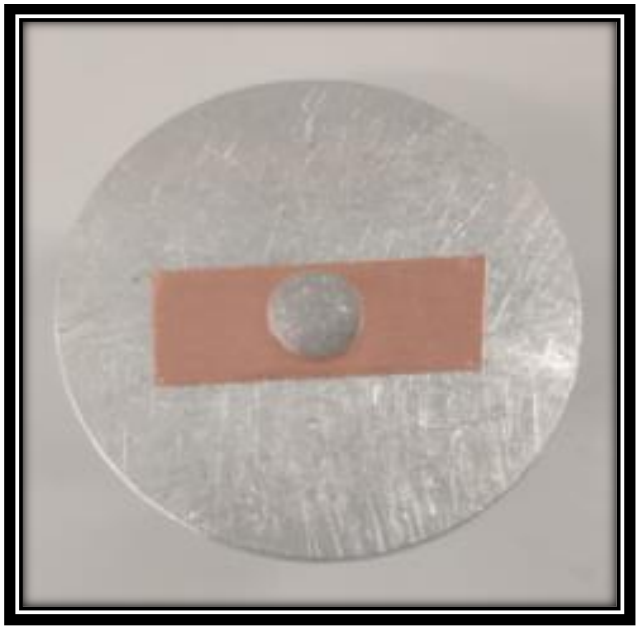

Figure 2.8: 50-50% of phosphor and glass ratio after sintering process

Therefore, further optimization of parameters was discussed and executed. The new parameters of the phosphor glass ratio were 5%, 10%, and 15% respectively. So, accordingly, the required amount of glass powder and phosphor powder was weighed in a balancing machine and put in a ball milling tank which consisted of metal balls, and the mixture of 5%,10%, and 15% was ball milled for 24 hours, respectively. The ball milling machine served the purpose of homogenous mixing of both glass and phosphor powder. After the ball milling machine process, the mixture was poured in a KBR pellet instrument and then phosphor in a glass sample was made with the help of a hydraulic press machine which is displayed in figure 2-9(c). The pressure required to prepare the sample was 4000 PSI (pound per square inch) and the powder was pressed in the machine for approximately 5 minutes to obtain the final circular disc-like
sample. Figure 2-9 displays the different steps involved to prepare the phosphor in the glass sample.

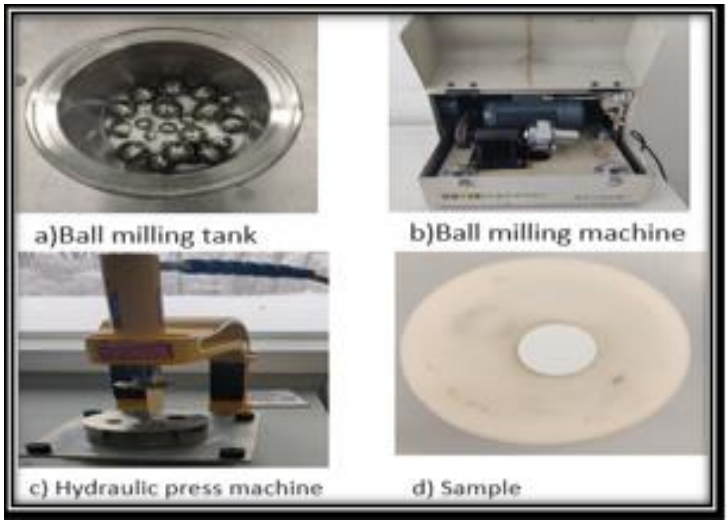

Figure 2-9: Fabrication process of Phosphor in Glass

Next, after the samples were made into a circular disc then they were sintered at the same temperature and time as used for 50-50% phosphor-glass ratio. But the result was not satisfactory for the above-mentioned sintering temperature as still showed an opaque nature. The image of the samples of 5%,10%, and 15% phosphor glass ratios are displayed in Figure 2-10.

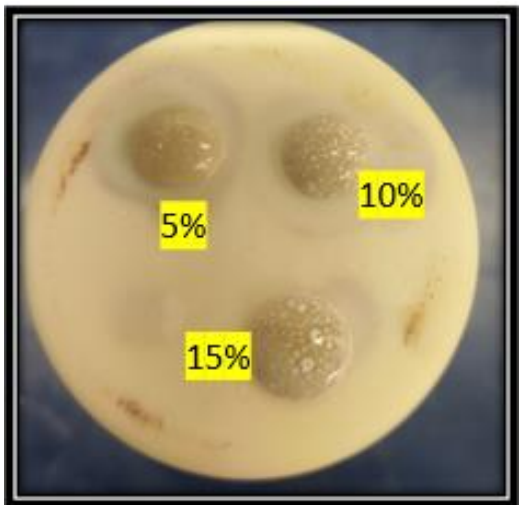

Figure 2-10: 5%,10% and 15% samples after sintering

Therefore, further optimization in the sintering time and temperature was done to get an expected result which is shown in table 2-3.

Sl.No	Sintering Temperature	Sintering Time
1.	25°C - 500°C	2 hours
2.	500°C - 500° C	2 hours
3	500°C - 900° C	4 hours
4	900°C- 900° C	2 hours
5	900°C-1100° C	2 hours
6	1100°C-1100°C	4 hours

Table 2-3: Details of Sintering time and temperature

2.5.2 Final sample after the optimized sintering process

The sample with 5%, 10%, and 15% content of phosphor in a glass after the sintering process is displayed below. The sample after undergoing the heat treatment became harder and durable, transparent, and a decrease in size in the sample was noticed. They were further examined using Scanning Electron Microscope.

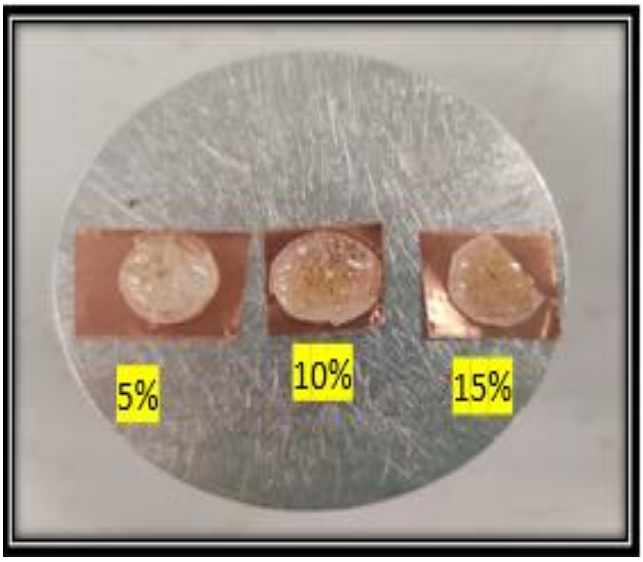

Figure 2-11: Sample 5%,10% and 15% after sintering process

Chapter 3 Instruments used for Characterization of Phosphor in Glass

Characterization of the 5%,10%, and 15% samples of phosphor in glass was done with Scanning Electron Microscope for analyzing the morphology and structure, fluorescence Spectrometer for testing excitation spectra, emission spectra ,UV-VIS for analyzing transmittance, a home-built set up for analyzing the quantum efficiency and also color purity of the samples was calculated with the recorded chromaticity co-ordinates. All these characterizations were done in the USN-lab facility.

3.1 Scanning Electron Microscope (SEM)

The basic principle that is involved in SEM also known as Scanning electron microscope is that it utilizes the help of an electron beam to scan on the sample which is kept on the sample holder. The electron beam is generated from either a tungsten filament or a field emission gun[18].

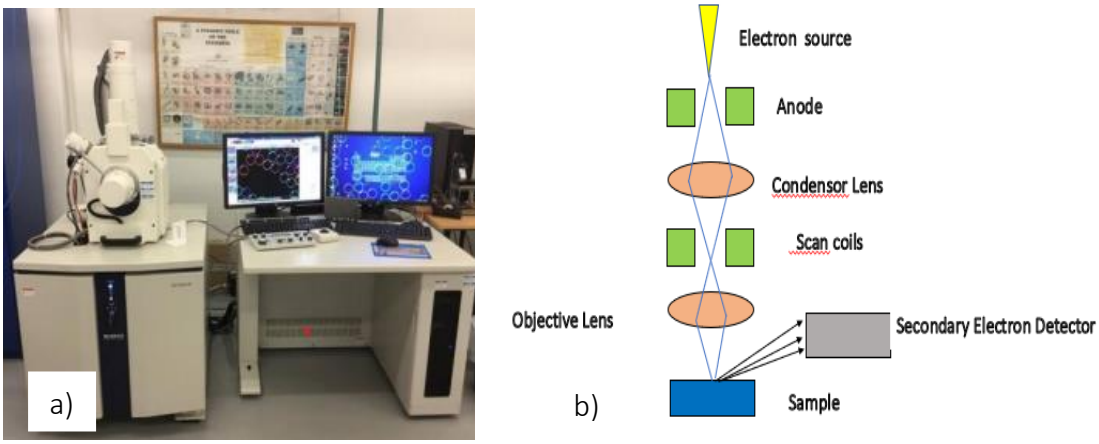

Figure 3-1: a) Hitachi SU3500 b) SEM Working Principle

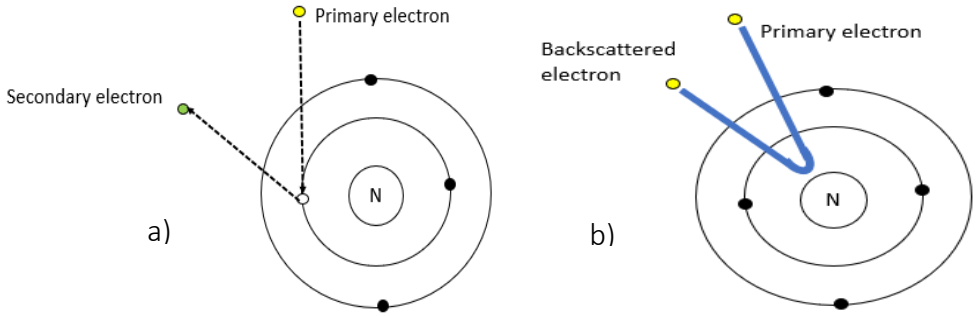

Figure 3-2: a) Secondary Electron b) Back-scattered electron

The bombarded electron beam travels via the electromagnetic lenses and scans the surface of the sample and other electrons (Secondary or BSE) are ejected from the sample which is detected by the detector and converts to the signal. These signals are displayed with SEM images and other details like topography, morphology, structure in the computer software. Secondary electrons provide the surface, topographical details of the material while back-scattered electrons provide more details about the depth of the material like composition existing in the sample.

Figure 3-1 a) displays the real lifetime SEM used for the project which is of the model Hitachi SU3500 and it provides magnification from 5 to 300,000x and accelerating voltages from 0.3 to 30kV and we can also analyze the 3D structure of the sample with the help of it.

3.2 Fluorescence Spectrometer for analyzing excitation and emission spectrum

For this project, an FS5 fluorescence spectrometer from Edinburgh Instruments has been utilized. The term Fluorescence originated during the year 1852 by Sir George G. Stokes when he noticed that a mineral by the name Fluorspar (calcium fluoride) was able to emit visible light(fluoresce) due to exposure to electromagnetic radiation[19]. Fluorescence is defined as the emission of light by a substance after absorption of electromagnetic radiation [19]. The principle of fluorescence spectroscopy works on the Jablonski principles[20] displayed in figure 3-3.

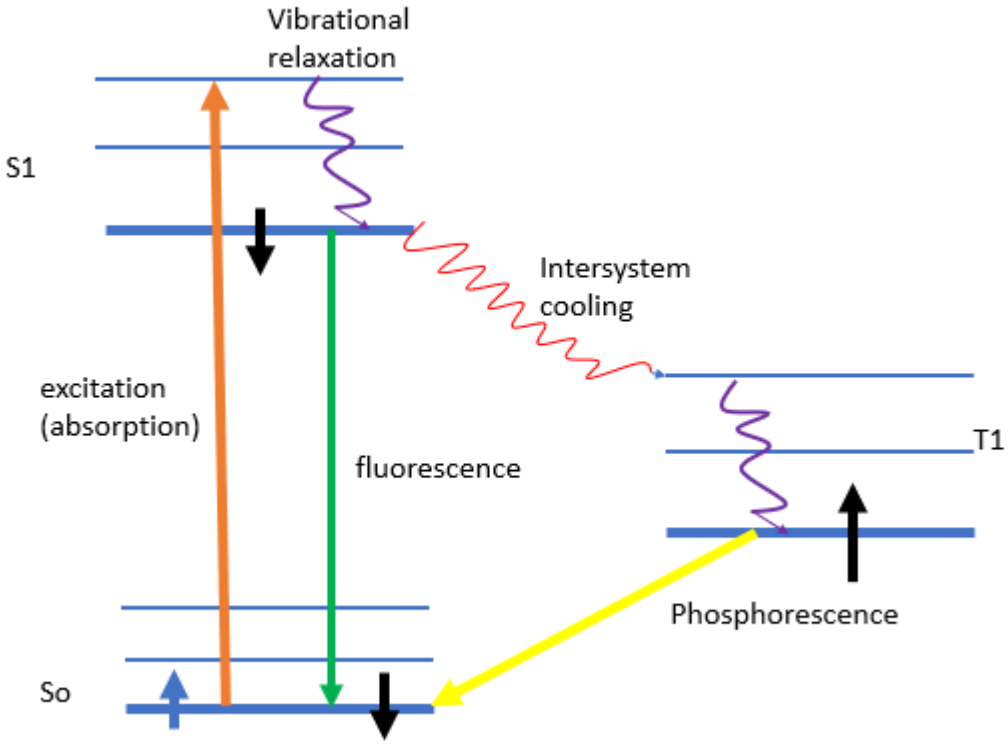

Figure 3-3: Jablonski principle

Fluorescence spectrometer consists of the following components as below[21]:

1. Light source: Xenon lamp is the source of light, and its function is to excite the atom or sample of use for the experiment. It produces a continuous spectrum.
2. Monochromator: Two types of monochromators are used where its function is to allow and pass only the specific required wavelength.

a) Excitation monochromator: passes the required radiation which is needed to excite the atoms/molecules.

b) Emission monochromator: passes the emitted radiation by the sample.

3. Sample holder: used to hold the sample in place firmly. Cuvette made up of glass or quartz is used as the sample holder.
4. Detector: it detects and converts the light energy into that of an electrical signal which is displayed in the computer or software used.
5. Computer/ Software: displays the graphical representation of excitation and emission spectrum.

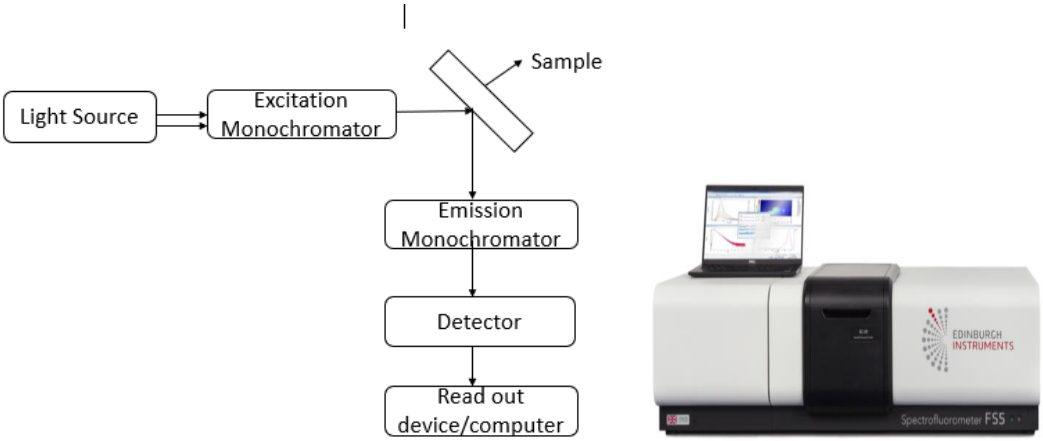

Figure 3-4: a) Working principle of Fluorescence spectrometer(left) b) FS5 spectrometer(right)

3.3 Quantum Efficiency

For the quantum efficiency, a homebuilt setup as displayed in Figures 3-5 was built and used for measuring the quantum efficiency of the samples.

It consists of a laser diode which is a xenon lamp source, an optical fiber through which the photons pass through, a temperature controller device, an integrating sphere and a computer for recording the quantum efficiency. Avantes 8.11 software was used for measuring the internal and external quantum efficiency.

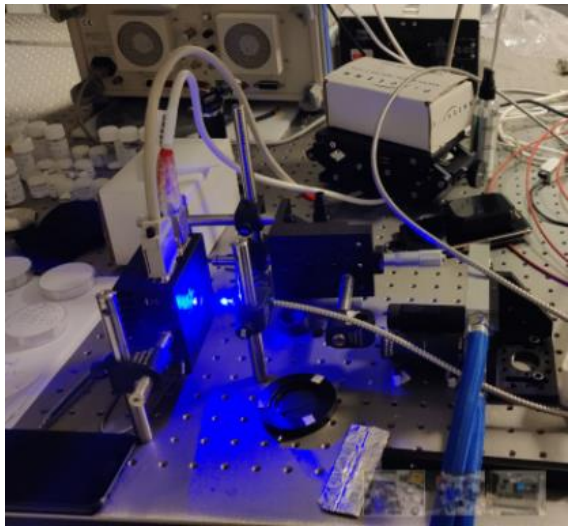

Figure 3-5: Homebuilt set up for quantum efficiency

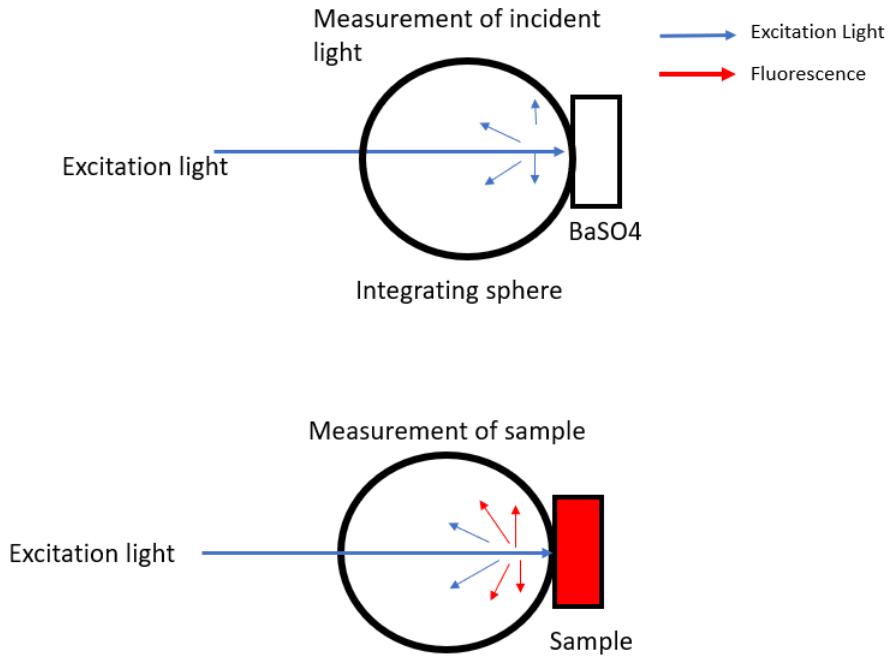

Figure 3-6: Working principle of quantum efficiency

Figure 3-6 shows working principle of quantum efficiency. It consists of 3 methods.

1. Excitation measurement: In this method no sample is inside the integrating sphere. We pass blue laser light with 450 nm wavelength and measure the intensity of excitation light. BaSo4 is used as white reference.

2. Measurement of emission spectrum:

In this step we place sample inside integrating sphere and measure the emitted light from the sample. We pass the blue laser light on the sample, and the sample absorbs most light. Some will not be absorbed. This is known as re-excitation.

3. Re-excited emission spectrum:

In this method we don't irradiate blue laser rays on the sample. Those light which was not absorbed by the sample is irradiated again on it by the integrating sphere. In this method we measure the re-excited emission spectrum.

3.4 UV-VIS Spectrophotometer

Figure 3-7 UV VIS 2600 instrument

UV-VIS 2600 from Shizmadzu, Japan was used to perform the transmittance characterization. It has an absorption wavelength of 185 nm to 900 nm. It utilises the UV-visible light as the primary source of energy.

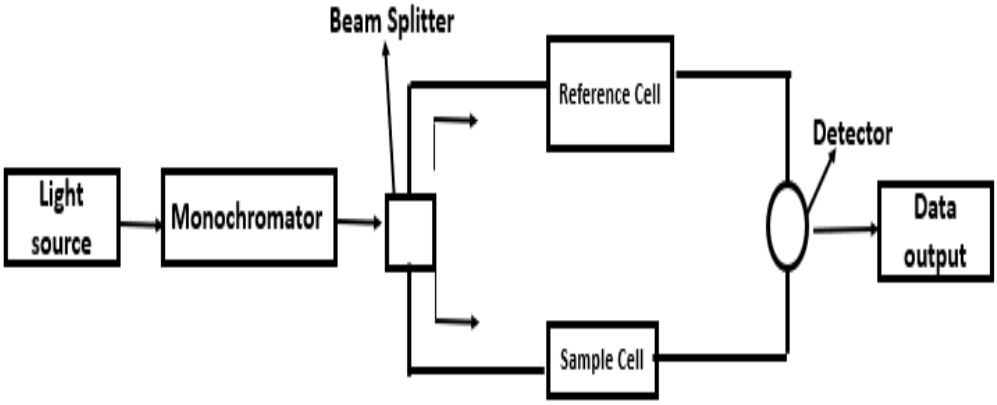

Figure 3-8 UV VIS Working principle

The working principle of UV-VIS is displayed in figure 2-18. When the light passes from the source to the monochromator which gets spread by diffraction grating. Thus, one single ray of light passes out towards the beam splitter. The beam splitter divides that single ray of light into two. One passes towards through the reference cell and the other through the sample cell. If the sample cell, generally a cuvette is used is

empty then 100% transmittance occurs[22]. This makes the transmittance of sample and reference equal, and it is detected by the detector and displayed in the data output.

Chapter 4 Results and Discussion

In this chapter, the experimental results obtained from different characterization techniques are studied and research understanding with regards to the data and results are presented.

4.1 Scanning electron microscope characterization

The figure below depicts the characterization results from scanning electron microscope for 5%, 10 %, and 15% phosphor to glass ratio samples respectively.

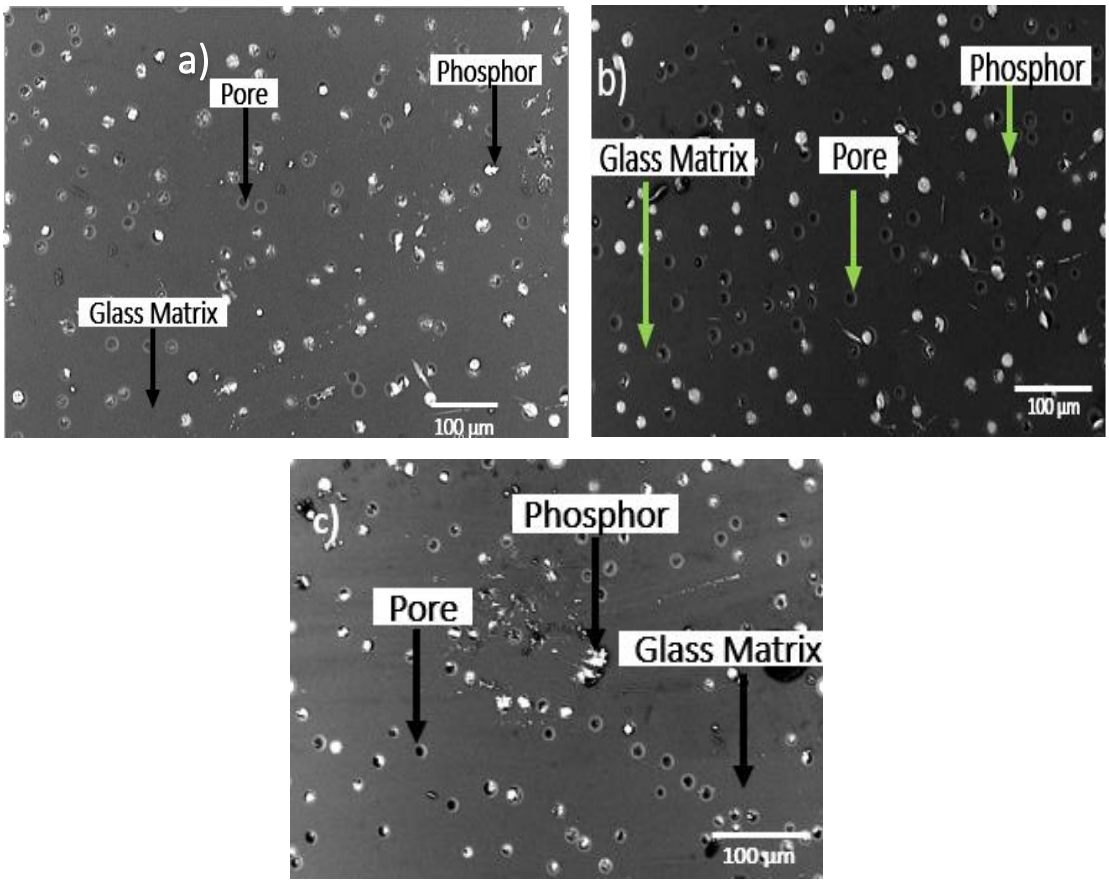

Figure 4-1: a) SEM image of 5% wt. phosphor b) 10%wt. phosphor c)15% wt. phosphor

Figure 4-1 a) illustrates the morphological image for the 5% wt. of phosphor. From this image, it can be inferred that there are air bubbles or voids created during the sintering

process. The pores in the samples were checked via the ImageJ software. There are various reasons and factors for the creation of pores in the phosphor in glass samples. The first factor as per the study is that some of the particles of the glass powder and phosphor particles which could not merge or combine leads to air trapped and it finally erupts as pores in the sample as displayed in the SEM image[23]. Another factor is the sintering temperature at which the sample is sintered [24]. The eruption of pores in the sample has a direct effect on the luminous efficacy and intensity of light[25] . It was inferred through research and experiment by Kim, S., et al. that the pores in the phosphor in glass sample lead to strong scattering of the light from the blue LED chip due to which the luminous efficacy and intensity of light get variations in the output result[25]. The phenomena of scattering of light from the pore are explained below with the figure 4-2 [25] which is inferred as per the experiment by the researchers Kim, S., et al. and as per what was understood from my part of studying and researching their experience of outcome out of this experiment.

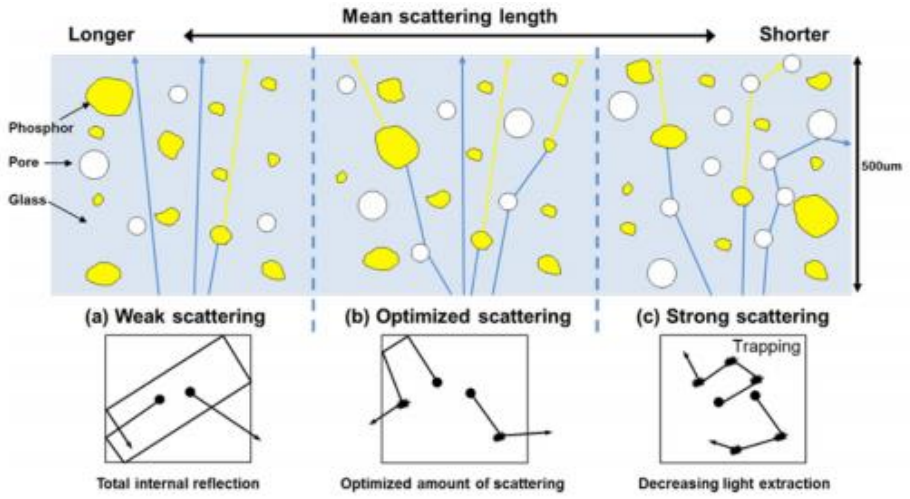

Figure 4-2: Different types of scattering of light from the Blue LED Chip [26]

From the above figure, there are three different types of scattering processes. The scattering process also determines the ability of the phosphor to absorb the blue rays which in turn gives different results of luminous efficacy. The increase in the number of pores leads to stronger scattering which leads to a huge decline/fall in the luminous efficacy and intensity of light[25].

1. Weak Scattering – In this type of scattering the mean scattering length is comparatively long due to which the phosphor can absorb much less from the blue light. Thus, total internal reflection occurs here [25]. This occurs because the interaction between the blue light and pore or phosphor is minimized.
2. Optimized Scattering – This type of scattering process gives the best result for luminous efficacy because the length of mean scattering is intermediate. In this case, the blue light is mostly absorbed by the phosphor [25]. Also, the interaction between the light and the pores and phosphor is controlled hence this phenomenon is considered an ideal type of scattering condition [25].
3. Strong Scattering – In this type of scattering there is a strong interaction between the blue light and the pores due to which the mean scattering length is decreased [2]. Hence, the blue light is much less absorbed by the phosphor thereby resulting in poor efficacy. Moreover, it was observed that the light emitted from the interaction between the phosphor and blue light is reabsorbed by the pores thereby decreasing the efficacy immensely [25].

From figure 4-2, it is understood that the availability of pores in the phosphor glass sample and its behavior have a significant effect on the luminous efficacy and efficiency of the white light production [25].

4.2 Results: Emission and Excitation spectrum

In this section, the emission and excitation spectrum of the three different samples of phosphor glass are analyzed and discussed.

4.2.1 Excitation Spectra for Phosphor glass with 5%,10%, and 15% ratio of phosphor over the glass

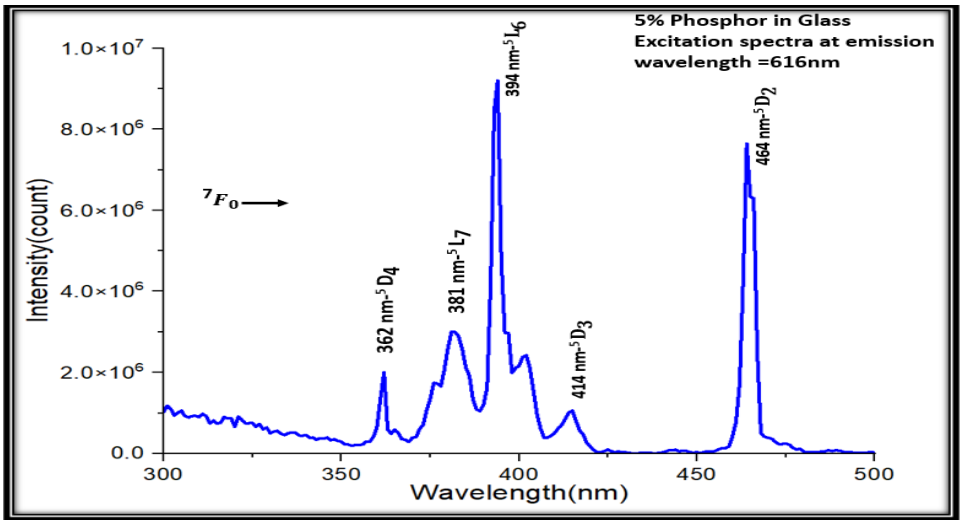

Figure 4-3: Excitation spectrum of 5% Phosphor in glass

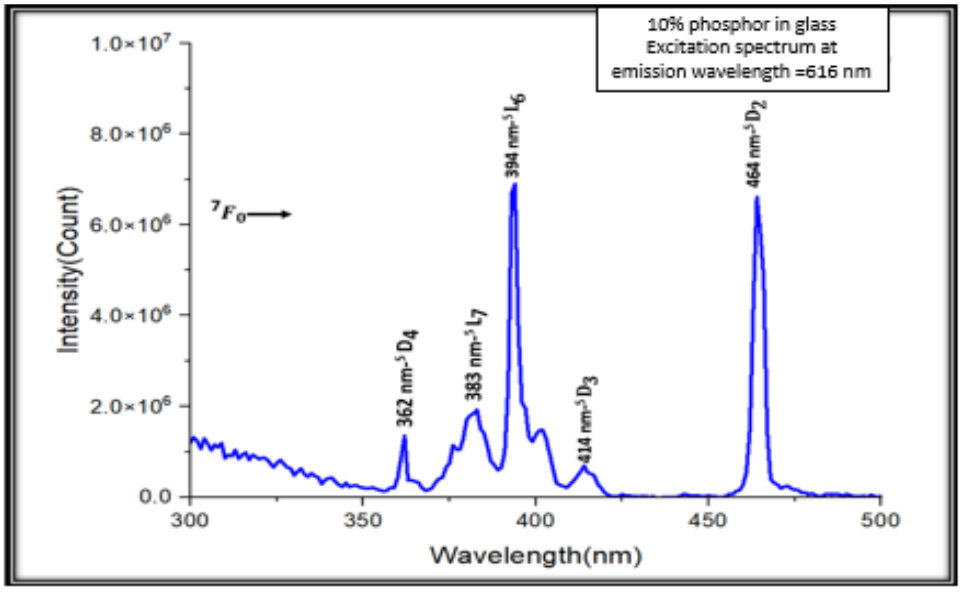

Figure 4-4: Excitation spectrum of 10% Phosphor in glass

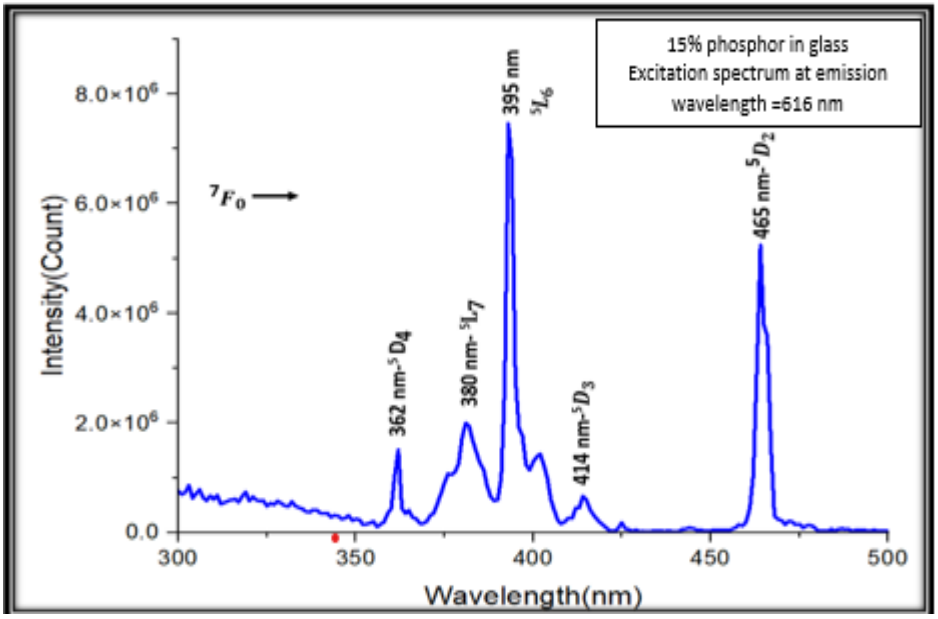

Figure 4-5: Excitation spectrum of 15% Phosphor in glass

In figure 4-3, the excitation spectrum obtained for the 5% phosphor glass sample is displayed. The excitation spectrum was measured at 616 nm of emission wavelength.

We see that there are a lot of narrow peaks from 350 nm-500 nm and among these peaks, the highest or most dominating peaks are in the wavelength of 394 nm, 464 nm, and 381 nm respectively. The narrow and sharp peaks from the wavelength of 350 nm – 500 nm are due to the intra-configurational f-f transition of trivalent europium ion i.e Eu^{3+} [26]. The dominating peaks at 394 nm are due to $^7F_0 \rightarrow {}^5L_6$ transition of Eu^{3+} and the least dominating or less intense peaks after 394 wavelength are 362 nm($^7F_0 \rightarrow {}^5D_4$), 381 nm($^7F_0 \rightarrow {}^5L_7$), and 414 nm($^7F_0 \rightarrow {}^5D_3$) respectively. The blue LED, UV rays are good sources for red emission of light with the help of the rare-earth ion Eu^{3+} [26].

Figures 4-4 and 4-5 illustrate the excitation spectrum of 10% and 15% of phosphor in glass respectively and figure 4-6 represents the excitation spectrum at 616 nm of emission for 5%, 10% and 15% samples. From figure 4-6 we see that and there is not much difference in the results of the different samples of 5,10 and 15% phosphor glass and similar peaks appear in all samples. Though the intensity in the 15% sample is the highest followed by 10% and then 5% phosphor in glass.

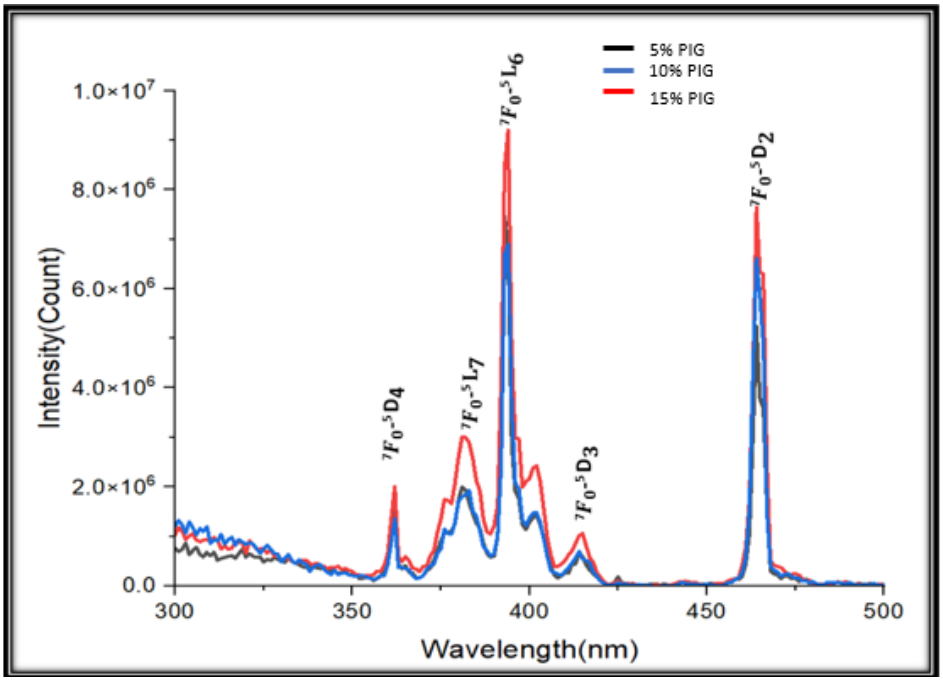

Figure 4-6: Combined excitation spectrum of 5%,10% and 15% Phosphor in glass

4.2.2 Emission Spectrum for Phosphor glass with 5%,10%, and 15% ratio of phosphor over the glass.

In this section, the emission spectra of 5%, 10%, and 15% ratios of phosphor in glass are analyzed. The emission spectra were measured with an excitation wavelength of 465 nm. Figures 4-7,4-8 and 4-9 represents the emission results and figure 4-10 represents the emission spectra for all three samples. We see that the dominating peak is present at 613 nm followed by comparatively small or weak peaks at 593 nm,654 nm, and 703 nm respectively. The dominating peak is due to the transition of $5\boldsymbol{D_0} - 7\boldsymbol{F_2}(613\ \text{nm})$ and the less intense peaks are due to $5\boldsymbol{D_0} - 7\boldsymbol{F_1}(593\ \text{nm})$, $5\boldsymbol{D_0} - 7\boldsymbol{F_3}(653\ \text{nm})$ and $5\boldsymbol{D_0} - 7\boldsymbol{F_4}(702\ \text{nm})$ respectively [27].As per the study, the transition of $5\ \boldsymbol{D_0} - 7\boldsymbol{F_1}$ is due to the magnetic dipole transition (MDT) which is parity allowed[28]. Due to this reason MDTs are not prone to be affected when there are alterations in the local environment surrounding Eu^{3+}. In contrast the transition $5\boldsymbol{D_0} - 7\boldsymbol{F_2}$ is due to electric dipole transition, which is forced, and has a large impact, and is

extremely prone to the changes surrounding local environment of Eu^{3+} [26]. The dependence of $\mathbf{5}\boldsymbol{D_0} - \mathbf{7}\boldsymbol{F_2}$ on the symmetry is termed as "hypersensitive transition [29].

The term "Asymmetry ratio" is the ratio of Electric dipole transition to the magnetic dipole transition [30].

Asymmetry Ratio = $\frac{\mathbf{EDT}}{\mathbf{MDT}}$ [31]

where EDT = is electric dipole transition [31]

MDT = is magnetic dipole transition [31]

The asymmetry ratio defines the alterations introduced in the environment around Eu^{3+} ions[31] . Initially, the MDT is dominating in the crystal site but with the addition of red activator ion i.e. Eu^{3+} the electric dipole transition overtakes and becomes dominant which results in a strong red emission of light [26].

As per Sahu, M., et al, the asymmetric environment at the lattice site is due to defect centers that exist around the Eu^{3+} ions [26]. Studies reported that these defect centres can decrease with the high temperature because an increase in temperature results in the decrease of the surface area thereby automatically resulting in a decrease of the defect sites too [26].

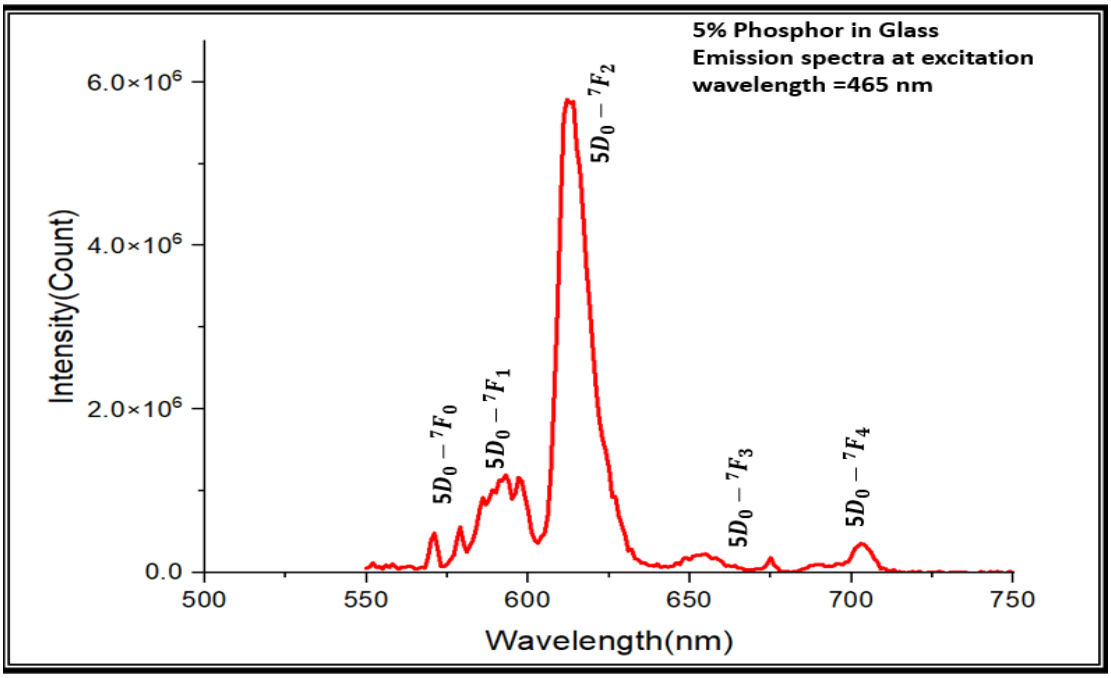

Figure 4-7: Emission spectrum of 5% Phosphor in glass

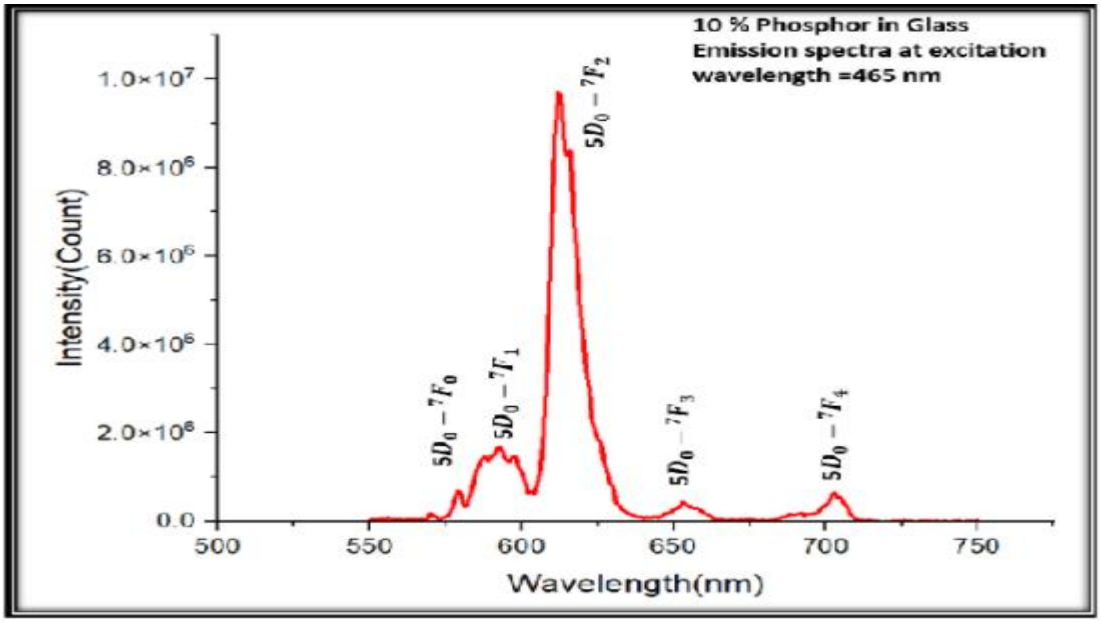

Figure 4-8: Emission spectrum of 10% Phosphor in glass

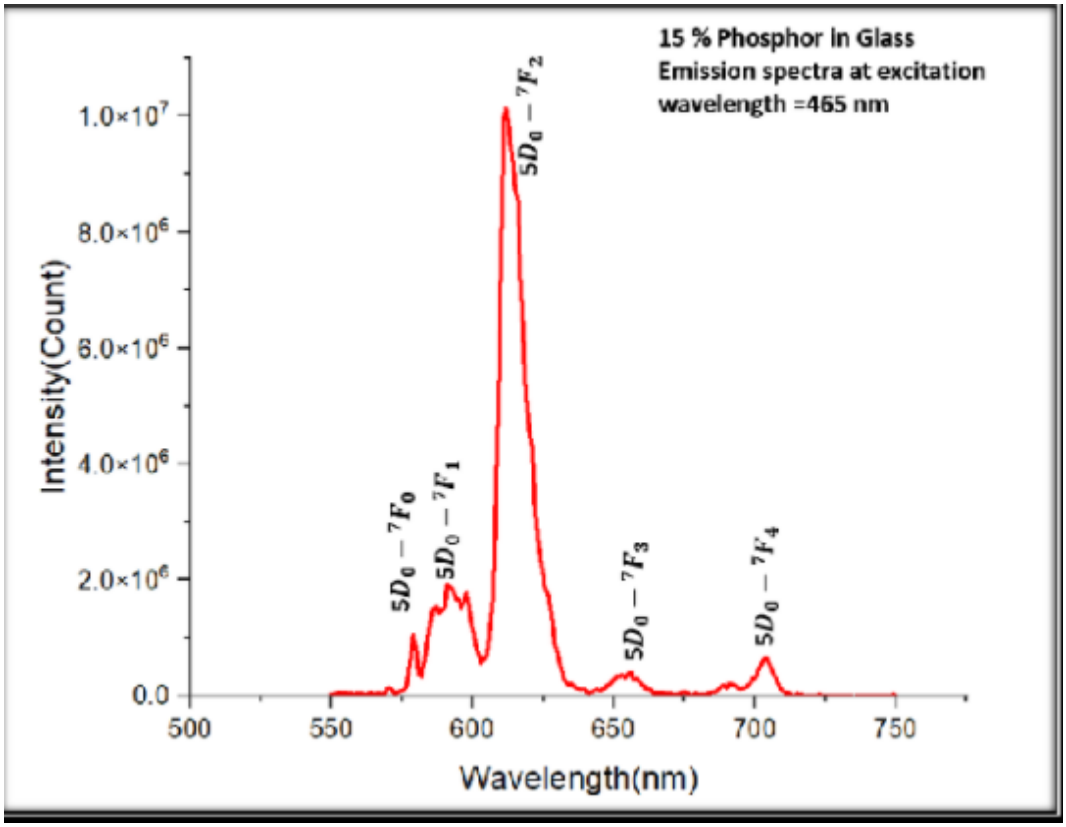

Figure 4-9: Emission spectrum of 15% Phosphor in glass

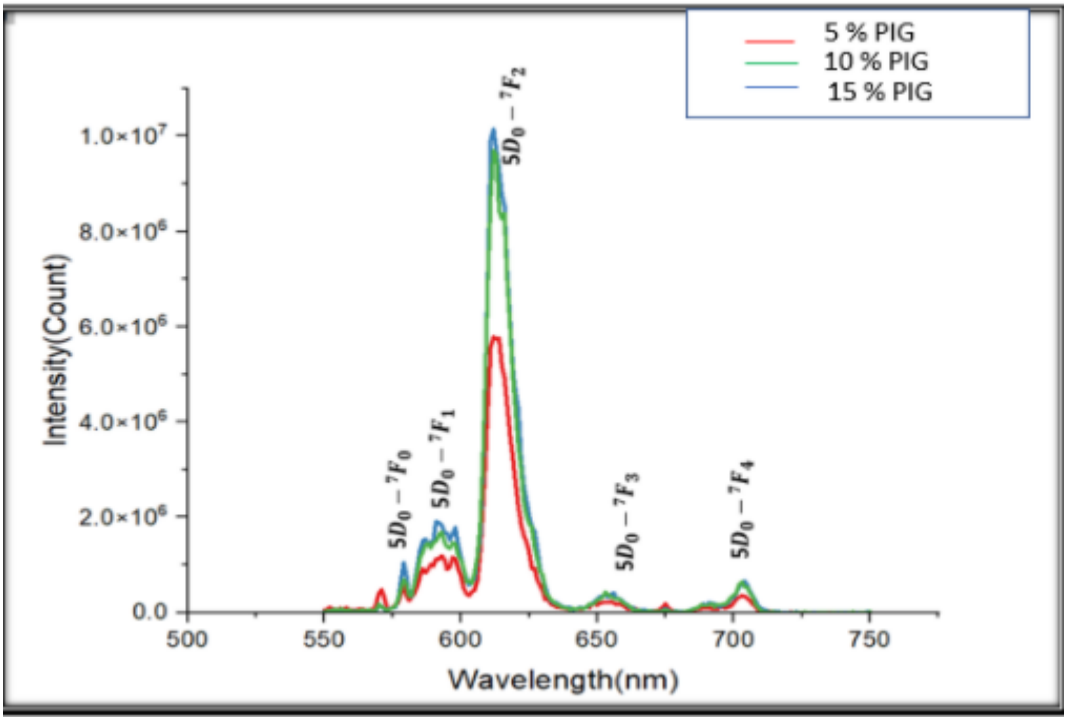

Figure 4-10: Combined emission spectra of 5%,10% and 15% Phosphor in glass

Figure 4-10 illustrates the combined emission spectra of all three samples of different ratios of 5%,10%, and 15% phosphor glass. The highest and dominating peak is seen at a wavelength of 613 nm and 15% phosphor glass had highest emission intensity.

4.3 Quantum Efficiency Result

Measurement of quantum efficiency for phosphor glass is an important characterization of the sample in luminescent technology [32]. Quantum efficiency (both Internal Quantum Efficiency and External Quantum Efficiency) of 5%, 10%, and 15% samples were taken and recorded in the tables below. They were measured under the excitation wavelength of 465nm. As, per D. Van der Heggen, et.al the quantum efficiency is dependent on the intensity of excitation wavelength, and as per the different excitation intensity applied the quantum yield or quantum efficiency also varies [33]. For our experiment quantum efficiency as per the phosphor, content was

Count of measurements performed	Sample	Internal Quantum Efficiency (%)	External Quantum Efficiency (%)
1.	5% Sample	35.4	28.9
2	5% Sample	34.2	27.2
3	5% Sample	35.2	28.5
4	5% Sample	35.3	28.9
5	5% Sample	32.8	28.4
Average result		**34.58**	**28.39**

Table 4-1: External and Internal Quantum Efficiency for 5% phosphor in glass sample

experimented. The internal and external quantum efficiency for all three samples with 5%, 10%, and 15% phosphor glass samples were taken under 465nm excitation wavelength. $BaSO_4$ was used as a white reference.

The results denote that there was an increase in both internal and external quantum efficiency with the increasing phosphor content sample. Measurements were taken five times with all samples and average results were recorded for accuracy. The highest

Internal quantum efficiency was for 15% phosphor glass sample with an internal quantum efficiency of 53.7% and external quantum efficiency of 37.16% respectively. 5% showed internal quantum efficiency of 34.58% and external quantum efficiency of 28.39. While 10% phosphor glass sample showed 42.5 internal quantum efficiency and external quantum efficiency of 33.2 respectively.

Count of measurements performed	Sample	Internal Quantum Efficiency	External Quantum Efficiency
1.	10% Sample	42.7	33.4
2	10% Sample	42.6	32.5
3	10% Sample	41.8	33.4
4	10% Sample	42.6	33.2
5	10% Sample	42.7	33.7
Average Result		**42.5**	**33.2**

Table 4-2: External and Internal Quantum Efficiency for 10% phosphor in glass sample

Count of measurements performed	Sample	Internal Quantum Efficiency	External Quantum Efficiency
1.	15% Sample	54.3	37.6
2	15% Sample	54.2	36.1
3	15% Sample	51.1	37.3
4	15% Sample	54.3	37.6
5	15% Sample	54.8	37.2
Average Result		**53.7**	**37.16**

Table 4-3: External and Internal Quantum Efficiency for 15% phosphor in glass sample

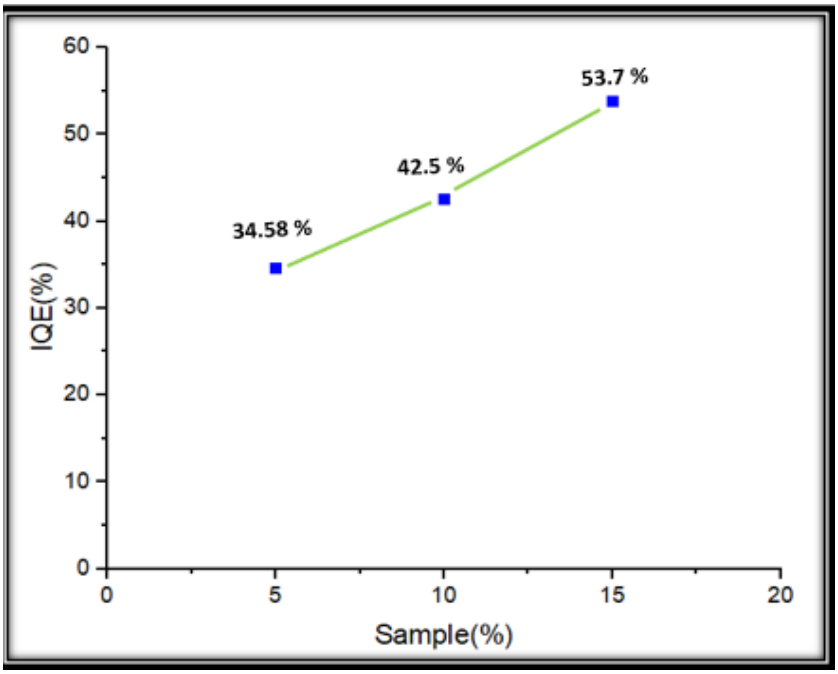

Figure 4.11: Internal quantum efficiency of 5%,10% and 15% phosphor glass samples

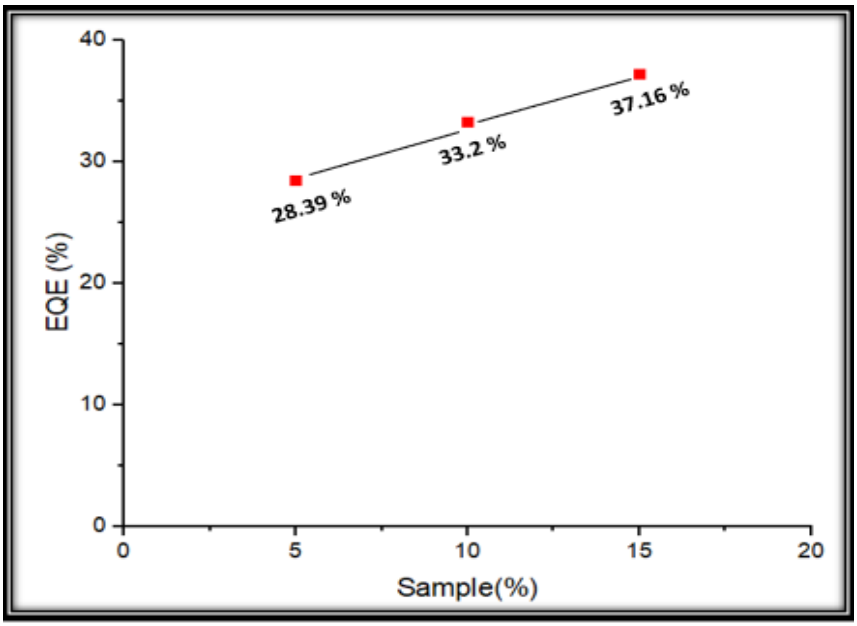

Figure 4.12: External quantum efficiency of 5%,10% and 15% phosphor glass samples

The graph for 5%, 10%, and 15% phosphor glass was plotted as per the internal and external quantum efficiency recorded.

4.4 UV-VIS Transmittance result and discussion

The transmittance of the phosphor glass sample was measured and recorded with the help of a UV-2600 spectrophotometer. The transmittance of the sample is dependent on factor enhanced scattering, densification which can influence the decrease in the transmittance %.

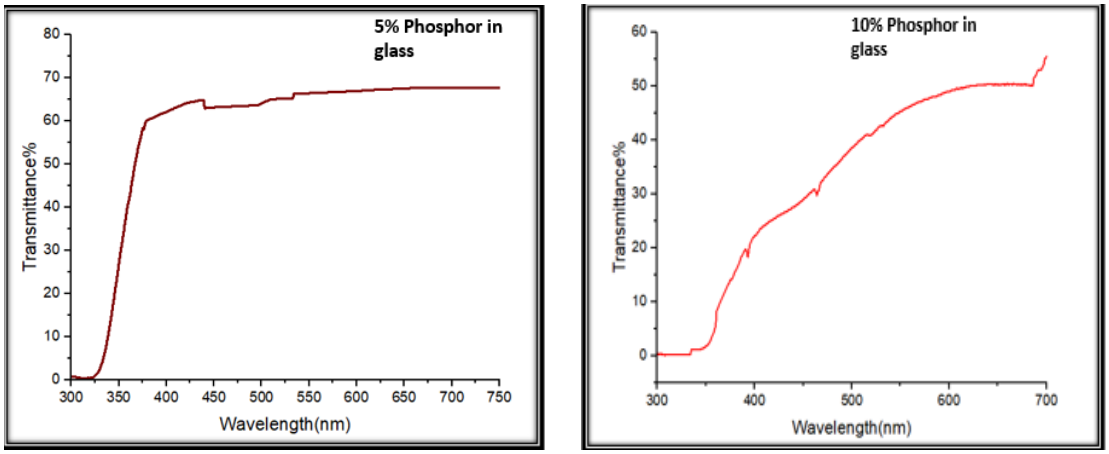

Figure 4-13: Transmittance of 5% phosphor glass(left), transmittance of 10% phosphor glass(right)

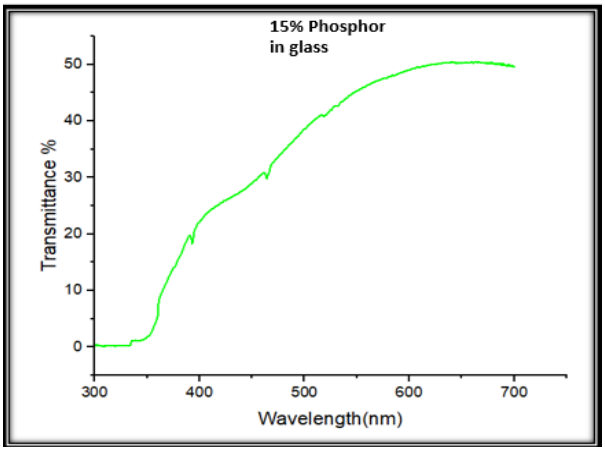

Figure 4-14: Transmittance of 15% phosphor glass

5% phosphor glass showed around 60% of transmittance. When the phosphor percentage was increased from 5% to 10% and 15% there was a decrease in the transmittance measurement of the samples.

In the transmittance measurement configuration, a decrease in the transmittance with an increasing phosphor percentage could attribute to the enhanced scattering of the phosphor powder in the sample.

4.5 Color Rendering Index study (CRI)

The color rendering index is an important metric to evaluate the efficiency and color purity of a white light-emitting diode. CRI which is abbreviated as color rendering index has its own standard i.e. CIE 1931. It has its ideal CRI coordinate for red phosphor at (x= 0.67, y=0.33) [34]. Figure 4-15,4-16 and 4-17 represents the chromaticity coordinates and the percentage of color purity. The results were generated at an excitation of 465 nm wavelength for different samples of phosphor glass content of 5%, 10%, and 15 % respectively.

The color purity calculation is done by the following formula:

$$\text{Color purity} = \frac{\sqrt{(X_s-X_i)^2 + (Y_s-Y_i)^2}}{\sqrt{(X_d-X_i)^2 + (Y_d-Y_i)^2}} \times 100\% \quad [37]$$

Where:

1. X_S = is Co-ordinate of the sample
2. Y_S = is Co-ordinate of the sample
3. X_i = is Co-ordinate of the standard white light-emitting diode
4. Y_i = is Co-ordinate of the standard white light-emitting diode
5. X_d = is Co-ordinate of the dominating wavelength
6. Y_d = is Co-ordinate of the dominating wavelength

Sl.No	Sample	Co-ordinate	Purity % of color
1	5%	(x=0.6434,y=.3562)	89%
2	10%	(x=0.6491,y=.3505)	91%
3	15%	(x=0.6509,y=.3487)	91%

Table 4-4: Color purity and CIE co-ordinates for 5%,10% and 15% at excitation wavelength 0f 465 nm

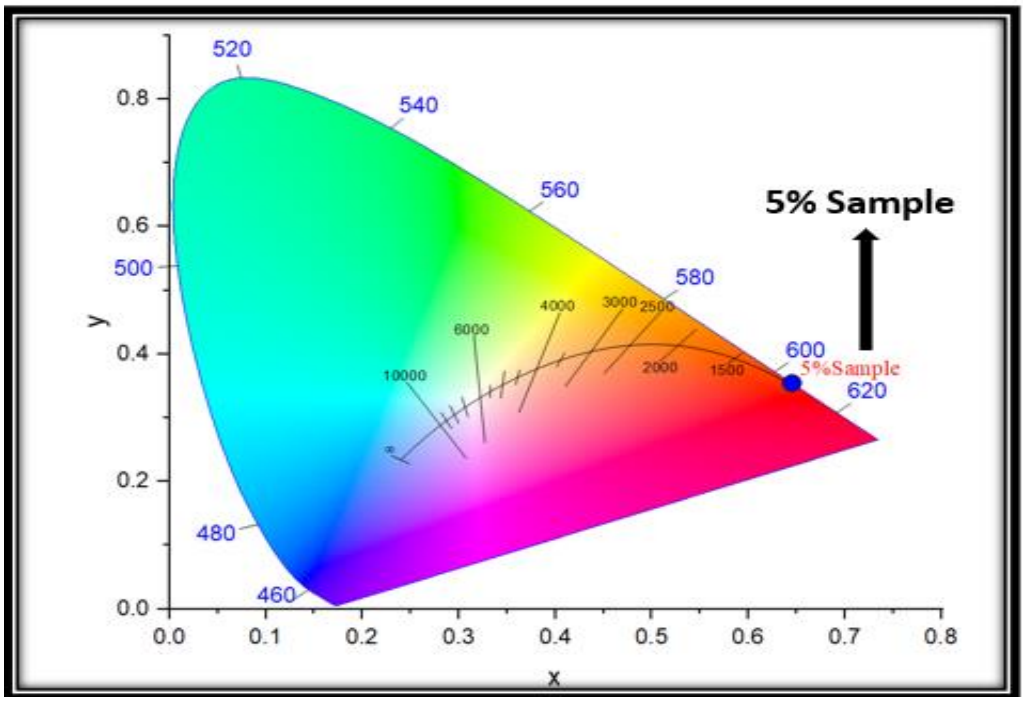

Figure 4-15: Representation of CIE co-ordinate point for 5% phosphor

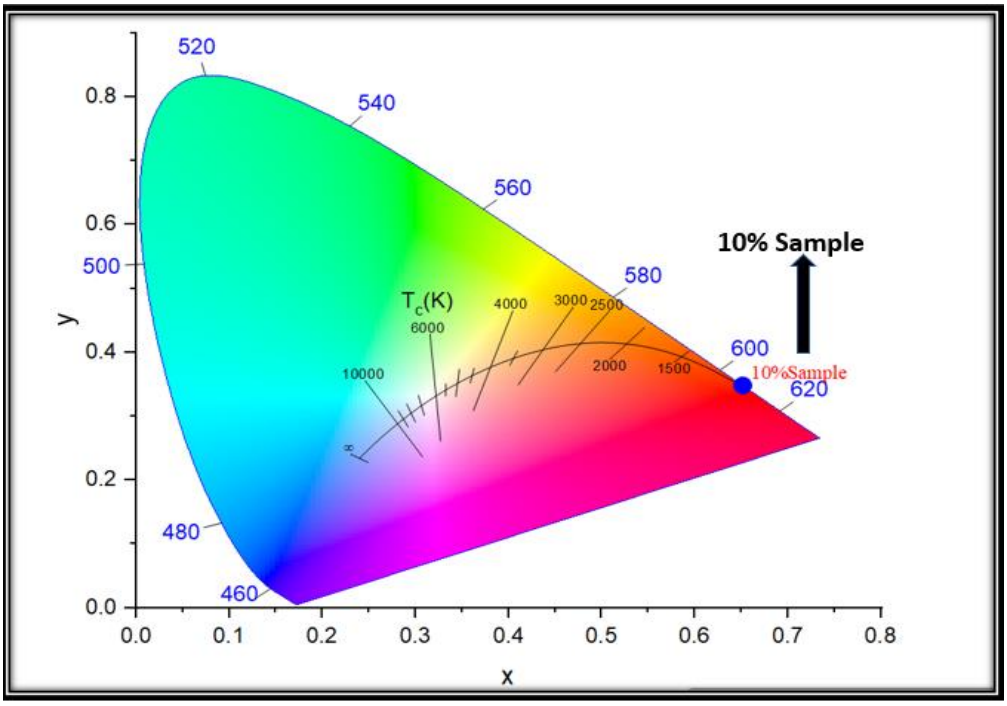

Figure 4-16: Representation of CIE co-ordinate point for 10% phosphor

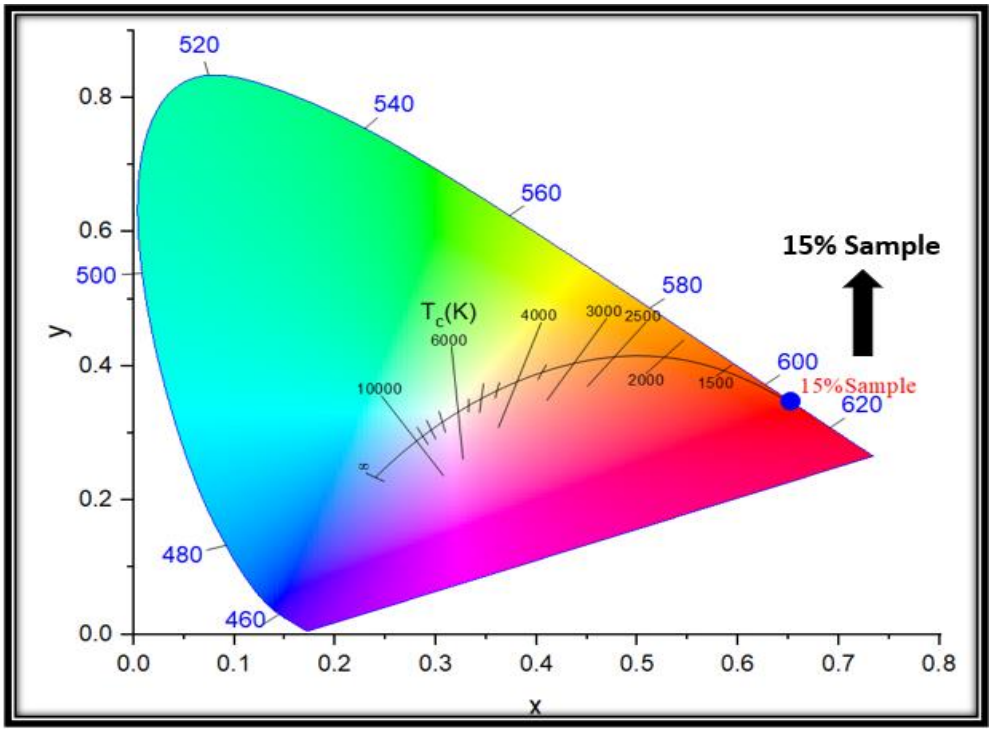

Figure 4-17: Representation of CIE co-ordinate point for 15% phosphor

From the above calculation, 5% phosphor glass sample 89% of color purity.

While the result for 10% and 15% of phosphor glass samples showed above 90% color purity. The excellent color purity percentage result denotes that the fabrication of red phosphor by sol-gel was successful in getting the required red color efficiency.

Figure 4-15, 4-16 and 4-17 represents the CIE coordinate plotting as per the emission Wavelength under the excitation of 465 nm wavelength. These chromaticity coordinates were obtained with the help of an FS5 fluorospectrometer.

4.6 Images of the sample under blue source of light

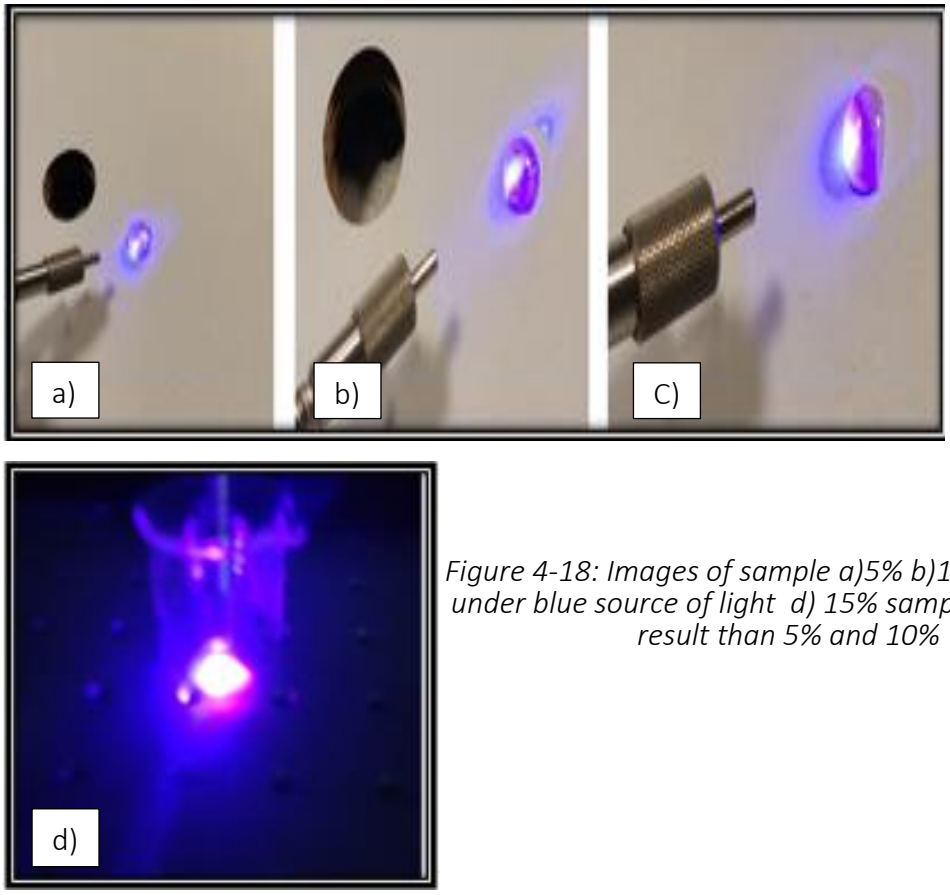

Figure 4-18: Images of sample a)5% b)10% and c)15% under blue source of light d) 15% sample with better result than 5% and 10%

5%, 10 %, and 15% samples were irradiated with blue laser light and the expected result should be violet color to achieve as a combination of blue and red should give violet. These results were achievable more with a 15% phosphor glass sample in comparison to the other 5% and 10% samples. The other two samples also displayed violet color as output but the result was better for the 15% sample.

4.7 Challenges faced

Due to the pandemic, there were lab restrictions that make limited access to the lab facility. Optimization of the fabrication parameters could not be performed as per the plan. Moreover, the XRD instrument had a technical error during the end of my final fabrication of samples. Therefore, characterization of my samples using XRD was not possible.

Chapter 5 Conclusion

In conclusion, fabrication of red phosphor powder, $Y(MoO_4)_3$ doped with $Eu^{3+}$was prepared by sol-gel method. The fabrication of phosphor in glass samples with different weight ratios of phosphor over glass (5%,10%, and 15%) was done. The morphology details and structure of the samples were investigated by SEM.

The sample with a weight ratio of 50%-50% phosphor over glass didn't give a better output as the phosphor powder has a too low density compared to the glass powder. The volume ratio of phosphor over glass is, therefore, larger. The SEM pictures for morphology analysis displayed the uneven distribution of phosphor powder which can greatly influence the color conversion and the transmitted output power. Therefore, the optimization for a better weight ratio of phosphor over glass has to be done. In addition, the sintering temperature is also modified. We used 5%, 10%, and 15% of phosphor along with an optimized sintering process, i.e., raised the temperature from 800° to 1100° Celsius for phosphor glass fabrication. The better results are achieved in terms of homogenous glass phase structure.

Photoluminescence was investigated and the excitation peak was dominating at 395 nm. This is due to $^7F_0 \rightarrow {}^5L_6$ transition of Eu^{3+}. The emission peak was dominating at 613 nm which is attributed to $5\boldsymbol{D_0} - 7\boldsymbol{F_2}$(EDT) transition.

Regarding quantum efficiency, with increasing phosphor in phosphor glass, both the internal and external quantum efficiency also increased. The sample of 15% phosphor has an internal quantum efficiency of 53.17 and external quantum efficiency of 37.16 respectively.

For the transmission measurement configuration, we have seen that the output power measured decreases with an increasing phosphor percentage in the phosphor glass.

The reason for such a phenomenon can be due to the enhanced scattering of the phosphor powder in the sample.

In addition, we found that color purity for a high percentage of phosphor glass is above 90% which is well demanded for the commercial products.

5.2 Future Recommendation

During this research, the goal was to fabricate red phosphor in glass with high performance.

Thus, it would be recommended for the following points to be incorporated.

1. Optimize the fabrication of phosphor in glass with research on the crystalline structure using XRD.
2. Combination of red phosphor with other phosphors. For instance, yellow phosphor to achieve enhanced brightness.
3. Study on the power saturation of the material.

Chapter 6 Reference

[1] Z. Kang, "Synthesis, characterization and application of luminescent quantum dots and microcrystalline phosphors," Georgia Institute of Technology, 2006.

[2] R. Boonsin, "Development of rare-earth-free phosphors for LED-based lighting devices," Université Blaise Pascal-Clermont-Ferrand II, 2016.

[3] L. Sangang, X. Xuan, J. Yu, H. Chengxiao, and Q. Kehui, "Synthesis and luminescence enhancement of CaLa0. 6 (MoO4) 1.9: Eu3+ red-emitting phosphors by Bi3+ doping for white LEDs," *Journal of Solid State Chemistry,* vol. 301, p. 122334, 2021.

[4] M. Balat, "Electricity from worldwide energy sources," *Energy Sources, Part B,* vol. 1, no. 4, pp. 395-412, 2006.

[5] S. L. l. solutions. "The Historical Evolution of Lighting." https://www.stouchlighting.com/blog/the-historical-evolution-of-lighting (accessed February,13, ,2021).

[6] I. T. l. a. c. FRANK GATTO & ASSOCIATES. "LED LIGHTING VS CONVENTIONAL LIGHTING[Online]." https://frankgattolighting.com/led-lighting-vs-conventional-lighting/. (accessed February 13, 2021).

[7] Wikipedia. "Phosphor [Online] " https://en.wikipedia.org/wiki/Phosphor. (accessed February 21, 2021).

[8] W. J. Chung and Y. H. Nam, "A review on phosphor in glass as a high power LED color converter," *ECS Journal of Solid State Science and Technology,* vol. 9, no. 1, p. 016010, 2019.

[9] V. K. Khanna, *Fundamentals of solid-state lighting: LEDs, OLEDs, and their applications in illumination and displays*. CRC press, 2019.

[10] K. Paisnik, G. Rang, and T. Rang, "Life-time characterization of LEDs," *Estonian Journal of Engineering,* vol. 17, no. 3, p. 241, 2011.

[11] S. D. Gupta and A. Agarwal, "Artificial lighting system for plant growth and development: Chronological advancement, working principles, and comparative assessment," in *Light emitting diodes for agriculture*: Springer, 2017, pp. 1-25.
[12] C. GLOBE. "Light Emitting Diode(LED)[Online] " https://circuitglobe.com/light-emitting-diode-led.html. (accessed March 2, 2021).
[13] J. Cho, J. H. Park, J. K. Kim, and E. F. Schubert, "White light‐emitting diodes: history, progress, and future," *Laser & photonics reviews,* vol. 11, no. 2, p. 1600147, 2017.
[14] K. Murthy and H. S. Virk, "Luminescence phenomena: an introduction," in *Defect and diffusion fórum*, 2014, vol. 347: Trans Tech Publ, pp. 1-34.
[15] C. R. Ronda, *Luminescence: from theory to applications*. John Wiley & Sons, 2007.
[16] S. M. S. e. al, "SYNTHESIS OF LUMINESCENT MATERIALS BY NUMEROUS METHODS " vol. 6, no. 1, 2019. [Online]. Available: http://troindia.in/journal/ijcesr/vol6iss1part3/1203-1210.pdf.
[17] X. Wang, "Preparation, synthesis and application of Sol-gel method," 2020. [Online]. Available: https://www.researchgate.net/publication/344942631_Preparation_synthesis_and_application_of_Sol-gel_method.
[18] H. Dixit, "A presentation on Scanning Electron Microscopy," ed, February,26,2018.
[19] B. Valeur and M. N. Berberan-Santos, "A brief history of fluorescence and phosphorescence before the emergence of quantum theory," *Journal of Chemical Education,* vol. 88, no. 6, pp. 731-738, 2011.
[20] Y. Ohnishi, "Fluorescence spectrophotometer," ed: Google Patents, 1974.
[21] Z. s. p. tutorials, "Fluorescence spectroscopy/flurometry/spectroflurometry," ed, 2018.
[22] H.-H. Perkampus, *UV-VIS Spectroscopy and its Applications*. Springer Science & Business Media, 2013.
[23] Y. Kim, S. Kim, F. Iqbal, H. Yie, and H. Kim, "Effect of transmittance on luminescence properties of phosphor-in-glass for LED packaging," *Optics express,* vol. 23, no. 3, pp. A43-A50, 2015.
[24] L. Zhou, L. Zhang, L. Wang, and Q. Zhang, "Concentration dependence of luminescent properties for Sr 2 TiO 4: Eu 3+ red phosphor and its charge compensation," *Journal of Nanomaterials,* vol. 2012, 2012.
[25] S. Kim, H. Yie, S. Choi, A. Sung, and H. Kim, "Pore characteristics for improving luminous efficacy of phosphor-in-glass," *Optics express,* vol. 23, no. 24, pp. A1499-A1511, 2015.
[26] M. Sahu, N. Phatak, and M. Saxena, "Exploring color tunable emission characteristics of Eu 3+-doped La 2 (MoO 4) 3 phosphors in the glass–ceramic form," *RSC Advances,* vol. 11, no. 28, pp. 17488-17497, 2021.
[27] P. Dang *et al.*, "Thermally stable and highly efficient red-emitting Eu 3+-doped Cs 3 GdGe 3 O 9 phosphors for WLEDs: non-concentration quenching and negative thermal expansion," *Light: Science & Applications,* vol. 10, no. 1, pp. 1-13, 2021.

[28] A. Parchur and R. Ningthoujam, "Behaviour of electric and magnetic dipole transitions of Eu 3+, 5 D 0⟶ 7 F 0 and Eu−O charge transfer band in Li+ co-doped YPO 4: Eu 3+," *RSC Advances,* vol. 2, no. 29, pp. 10859-10868, 2012.
[29] B. Bondzior and P. J. Dereń, "The role of hypersensitive transition in Eu3+ optical probe for site symmetry determination in BaScBO-SrScBO solid-solution phosphor," *Journal of Luminescence,* vol. 201, pp. 298-302, 2018.
[30] I. E. Kolesnikov *et al.*, "Asymmetry ratio as a parameter of Eu3+ local environment in phosphors," *Journal of Rare Earths,* vol. 36, no. 5, pp. 474-481, 2018.
[31] P. Jena, S. K. Gupta, K. Sudarshan, N. Pathak, and A. K. Singh, "A step towards synthesizing unique UV and visible light excitable AWO 4: Eu 3+(A= Ca and Sr) nanophosphors using high energy ball milling method: luminescence differences in going from Ca 2+⟶ Sr 2+," *Journal of Materials Science: Materials in Electronics,* vol. 29, no. 16, pp. 13751-13765, 2018.
[32] M. Janulevicius *et al.*, "Luminescence and luminescence quenching of highly efficient Y 2 Mo 4 O 15: Eu 3+ phosphors and ceramics," *Scientific reports,* vol. 6, no. 1, pp. 1-12, 2016.
[33] D. Van der Heggen, J. J. Joos, and P. F. Smet, "Importance of evaluating the intensity dependency of the quantum efficiency: impact on LEDs and persistent phosphors," *ACS Photonics,* vol. 5, no. 11, pp. 4529-4537, 2018.
[34] C. Stream. "Understanding CIE 1931 chromaticity." https://cascadestream.com/2017/06/18/understanding-cie-1931-chromaticity/ (accessed 2021).